NAVORD REPORT 3922

FC

PHOTOCONDUCTIVITY IN LEAD SELENIDE

21 MAY 1955

U. S. NAVAL ORDNANCE LABORATORY
WHITE OAK, MARYLAND

NAVORD Report 3922

PHOTOCONDUCTIVITY IN LEAD SELENIDE

Prepared by:

James N. Humphrey

ABSTRACT: The mechanism of photoconductivity in thin films of lead selenide has been investigated through the use of starting materials prepared in various ways, by using various sensitizing agents, and by varying the film thickness and the conditions of preparation of the films. The range of conditions producing sensitivity as well as the differences in sensitivity are used to formulate a model for the mechanism.

The sensitizing agents used were oxygen, sulfur, selenium, and the halogens. Each sensitizer was found to act as an acceptor impurity, causing the resistance of an n-type sample to increase to a maximum and then decrease, the film becoming p-type at the condition of maximum resistance. At 25°C measurable sensitivity (with a time constant of about 1 microsecond) results only if oxygen has been introduced. At -195°C all sensitizers tested produced sensitivity with time constants about 15 microseconds: oxygen-treated films showed both this time constant and one of about 5 milliseconds.

It is believed that within the crystallites there exist recombination centers which quickly return to the valence band any electrons elevated by absorbed radiation. Each of the sensitizers is capable of producing surface states which are

responsible for the resistance variation and change of carrier sign. In addition, oxygen atoms can enter the crystallites interstitially, forming electron traps. Thus any optically elevated electrons can be trapped, and recombination with a free hole delayed. This results in an increase of photoconductivity (the free holes carrying the photocurrent), with a time constant equal to the time for escape of an electron from interstitial oxygen.

At -195°C the fast (15 microsecond) response is identified with the direct recombination process, while the 5 millisecond response time is identified with the escape of the electron from the interstitial oxygen. At 25°C the observed response time ($\sim$ 1 microsecond) is identified with the escape from the oxygen.

The relation between absorption coefficient, film thickness, and sensitivity is examined. Present sensitivity data agree with theoretical expressions and certain published absorption data, but disagree with published absorption curves for short wavelengths, calculated from reflectivity measurements. A method of estimating the wavelength dependence of band-to-band absorption is suggested.

U. S. NAVAL ORDNANCE LABORATORY
WHITE OAK, MARYLAND

NAVORD Report 3922 21 May 1955

This report describes the results of an investigation of the sensitization of photoconductivity in lead selenide films. A theory of the mechanism producing photoconductivity is developed from the experimental results. The work is a result of the combined interest of the Naval Ordnance Laboratory and the University of Maryland in semiconductor research. This report has been submitted as a thesis, in substantially the same form, to the University of Maryland in partial fulfillment of the requirements for the Ph.D. degree in physics. The work was performed jointly under FR-21-55 and A8e-3-1-55. This report is intended for information only.

JOHN T. HAYWARD
Captain, USN
Commander

D. F. Bleil

D. F. BLEIL
By direction

CONTENTS

LIST OF ILLUSTRATIONS

CHAPTER I

INTRODUCTION

SECTION A. The Lead Compound Semiconductors

When electromagnetic radiation is absorbed by certain materials the electrical conductivity may be changed. If this change occurs by direct interaction of the radiation with the electronic system of the material, without first raising its temperature, the process is called photoconductivity. If the change occurs only because of a change in temperature produced, the process is called a bolometric effect.

From the point of view of physics photoconductivity has a twofold importance. First of all, it represents a source of information about electronic processes in solids, some of which cannot easily be obtained by other measurements. In this way, it serves as a tool useful in furthering our understanding of the fundamental properties of solids. On the other hand, it has direct application as a method of detecting radiation and, hence, can profitably be studied for the purpose of application to specific instruments or devices, such as spectrometers. It is from the former point of view that the present investigation has been carried out.

The semiconductors PbS, PbSe, and PbTe form a family having quite similar properties, most of which show progressive changes

as we pass through the family in the direction of increasing atomic number. In particular, they all can be processed to make them photoconductive in the visible and near infrared, at least at reduced temperatures. The index of refraction, lattice spacing, and molar heat capacity all increase as we go from smaller to larger atomic numbers. The limits of the spectral region in which photoconductivity takes place do not follow this order, however. The response of lead selenide extends to longer wavelengths than does that of either lead sulfide or lead telluride.

Because of the similarities it is believed that the process of photoconductivity will ultimately be described in terms of models which are essentially the same for the three materials, but perhaps showing some secondary differences. Accordingly, we will refer frequently to information and conclusions drawn from studies of the other members of the family. Because of the peculiar inversion of the spectral limits, considerable interest in lead selenide has been aroused.

At the present time there is no general agreement among the workers in this field as to the mechanism of photoconductivity in these materials. There are two general models which are under consideration. There are also numerous theories as to the details to be included in each of these general models.

In the case of PbSe the experimental difficulties in preparing and retaining sensitive films are great. Furthermore,

there is some disagreement among those who have prepared sensitive films as to the effect of certain parameters on the properties of the PbSe.

SECTION B. Photoconductivity and the Band Theory

According to the band theory of solids the energy levels observed in an atomic system are broadened out into energy bands when a large number of the atoms are condensed to form a solid. The ground state levels of the valence electrons form a band in which all states are occupied at absolute zero, if the solid is an insulator or semiconductor. This is called the valence or full band. The first excited states of the atomic valence electrons form a band which is normally empty at absolute zero. This is the conduction band. The energy difference between the bottom of the conduction band and the top of the full band is called the energy gap or forbidden band and designated by ΔE.

In the case of metals the valence electrons form a band which is not full at absolute zero.

If there are foreign atoms, stoichiometric deviations, or crystal imperfections in the solid, there will be extra permitted energy levels which normally will not fall within the same limits as those of the perfect solid; they are usually near to but separated from either the valence or conduction band. They are called impurity levels.

Figs. 1a and 1b show these two principal bands and two types of impurity levels. Some foreign atoms normally tend to release electrons to the conduction band at temperatures above 0°K. These are called donor impurities. A semiconductor containing such impurities will be n-type (n for negative carrier), as in Fig. 1a. The position of the level, ΔE_D in Fig. 1d, is measured from the bottom of the conduction band.

Other atoms tend to attract electrons away from the valence band. They are called acceptor impurities, and their inclusion produces p-type material, Fig. 1b. Their position ΔE_A is measured from the top of the valence band.

In case both donor and acceptor impurities are present the sign of the carrier will correspond to the impurity type present in the larger numbers. Certain exceptional cases in which this is not true exist but do not concern us here.

If the temperature of a semiconductor is raised above absolute zero two effects occur. First the impurity levels are ionized, donors giving electrons to the conduction band and acceptors taking electrons from the valence band (i.e., creating holes in the full band). At higher temperatures electrons are raised directly from the valence band to the conduction band. Since conductivity is $\sigma = \sum_j n_j e \mu_j$ both of these processes tend to raise the conductivity of the semiconductor. Here n_j and μ_j are the concentration and mobility (velocity per unit applied electric field) of the carriers of type j (holes and electrons

in the case of pure electronic conductivity).

The distribution of the electrons among the various permitted energy levels and bands at a particular temperature T°K is given by the Fermi-Dirac distribution function $\underline{f}$. This function is defined as the probability that at thermal equilibrium a quantum state of energy E is occupied by an electron. We further define that energy E_f for which $\underline{f}$ takes on the value 1/2, as the "Fermi level". The distribution function $\underline{f}$ is given by

$$\underline{f} = \underline{f}[(E - E_f)/kT] = \frac{1}{1 + e^{(E-E_f)/kT}} \qquad (1)$$

The number of electrons at a particular energy E is the product of the distribution function $\underline{f}$ and the function n(E) giving the density of states (possible energy levels).

The position of the Fermi level is a function of the intrinsic properties as well as of the impurities. In intrinsic material E_f will be essentially half way between the valence and conduction bands. The addition of donor type impurities raises E_f, while acceptor levels lower E_f. The total number of electrons is given by the integral $\int f(E)n(E)dE$ over all the possible states; for a given sample the integral must be a constant independent of temperature and of the distribution of states. An increase of temperature will move the Fermi level towards the center of the forbidden band, in the usual case, since the value of $e^{(E-E_f)/kt}$ moves towards unity as T increases.

Another way the number of conducting holes and electrons can be increased is by the action of light. Figs. 1c and 1d illustrate the mechanisms. If radiation of energy E_r falls on the lattice it may be absorbed. If $E_r \geq \Delta E$ the energy of a photon can be imparted to an electron in the valence band, increasing the electron energy by E_r. Accordingly a free "electron-hole pair" is produced and the photon disappears. For the time during which the electron is able to remain in the conduction band the conductivity $\sigma = \sum_j n_j e \mu_j$ is greater than its value in absence of the radiation. This increase in conductivity is termed photoconductivity. The deviation from the equilibrium concentration $\bar{n}$ of carriers is given in the case of low illumination by

$$n - \bar{n} = \Delta n = \alpha I \tau \qquad (2)$$

where τ is the recombination time constant, I is the number of photons incident per cm^2 per sec., and α is the absorption coefficient. The differential equation for which this is the solution is given in the Appendix.

A diagrammatic representation of a photoconductive sample and the equipment needed to observe the photoconductive response is shown in Fig. 2. The decrease of resistance on illumination produces an increase in current through the ammeter. The relative change of current $\Delta i/\bar{i}$ is a measure of the photoconductive

FIG. 1
SEMICONDUCTOR ENERGY BANDS AND OPTICAL EXCITATION

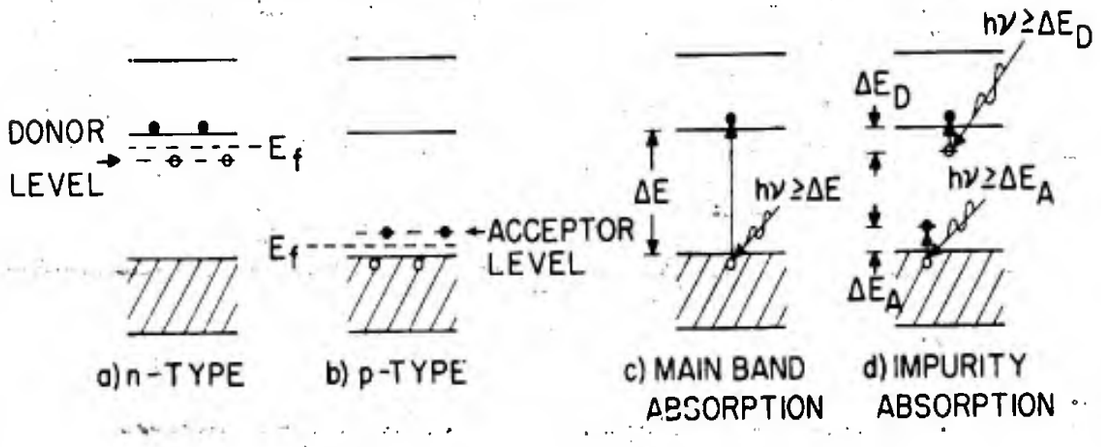

FIG. 2
PHOTOCONDUCTIVE CELL AND METHOD
FOR OBSERVING RESPONSE
(DIAGRAMMATIC)

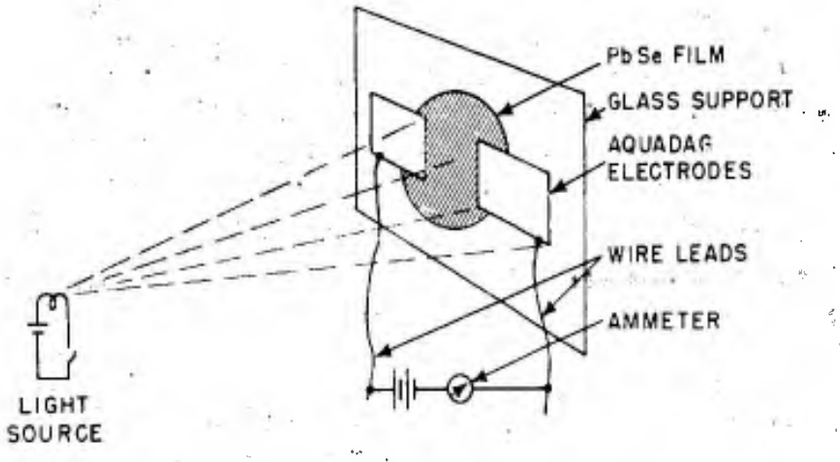

sensitivity, which may be more completely defined as the fractional change in conductivity $\Delta G/\bar{G}$ for unit incident radiant intensity.

Evidently for radiation of energy $E_r < \Delta E$ this absorption mechanism (called band-to-band or main band absorption) does not exist. Other mechanisms do exist (free-electron absorption, for example) in this energy region, but they are very much weaker than band-to-band absorption, in pure crystals. Thus, the wavelength at which an "absorption edge" (a sharp drop in absorption with increasing wavelength) occurs may be identified with the energy gap. An advantage of the use of this phenomenon for measuring ΔE is that it can be done at constant temperature, so any change in ΔE with T may be determined.

At temperatures sufficiently low that the impurity levels are not ionized (i.e., each donor level still contains its electron and the acceptor levels are empty), light of energy $E \geq \Delta E_D$ can serve to ionize the donor levels, and light of energy $E \geq \Delta E_A$ can serve to ionize the acceptor levels. The resulting increased conductivity is termed impurity photoconductivity. It is also apparent that the presence of such impurities can obscure the main absorption edge.

It should be noted that the presence of illumination on a sample means that the sample is no longer in thermal equilibrium with its surroundings; thus a somewhat different distribution function exists in this case.

SECTION C. Properties of PbSe

Lead selenide is a shiny, gray, opaque, crystalline semiconductor of density 8.10 g/cc. Its crystal structure is that of rock-salt, with a lattice spacing of 6.14 A^{o}. The binding is believed to be partially ionic and partially covalent. The solid melts at 1065°C and sublimes in vacuum at 450°C. The forbidden energy gap is about 0.25 ev, and the index of refraction is 4.54. In the form of properly sensitized thin films PbSe shows photoconductivity in the visible and near infrared, to a limit of 5 microns at room temperature and 7 microns at nitrogen temperature.

The earliest measurement of the conductivity of PbSe is that of Bauer[1]. He prepared crystals by various methods, and measured the Hall effect, thermoelectric power, and resistivity. His resistivity vs. temperature data for samples with impurity concentrations from 2×10^{17} to 2×10^{19} cm^{-3} has been replotted as $\log \rho$ vs. 1/T in Fig. 3, to display any activation energies present. A calculated intrinsic resistivity limit is given which is based on his mobility values and the most recent value (0.25 ev) of ΔE. The effective mass m_e^* of the carrier is assumed to be equal to the mass m_e of a free electron. All of his curves except that for sample #4 agree fairly well in character with the best modern data on PbS crystals (Brebrick and Scanlon[2]). Their PbS curves have been analyzed in terms of impurity concentration and a temperature dependence of mobility[3]. The ratio between the

resistivities of any two samples at the same temperature (from -195°C to 25°C) agrees with the ratio of the concentrations of carriers as indicated by Hall measurements, showing the mobility to be independent of impurity scattering. Further analysis accounted for the temperature dependence of mobility in this range in terms of lattice vibration modes.

At about the same time Eisenmann[4] and Hintenberger[5] reported experiments in which they were able to change the resistance and carrier sign of PbS by heat treatment in vacuum or in sulfur vapor. Hintenberger showed that stoichiometric PbS films exhibit a minimum conductivity; deviations either to excess lead or excess sulfur increase the conductivity. This he interpreted in terms of impurity conductivity as described above. In a second paper[6] he investigated the effects of O_2, N_2, H_2, and A on PbS and reported that O_2 (or air) produced results exactly analogous to those produced by sulfur treatment; n-type material showed an increased resistance as a result of baking in oxygen, followed by a decrease in resistance and change to p-type on continued baking. He was able to pump out the oxygen at high temperatures, obtaining the original low resistance n-type condition. He suggested that the oxygen goes in interstitially when baked to no higher than 170°C, but substitutionally fills sulfur vacancies when baked to 350°C.

During World War II the Germans discovered the photoconductive properties of PbSe. No details of their work were

published, however. In 1946 the Admiralty Research Laboratory in England instituted an investigation of photoconductivity in PbS, PbSe, and PbTe. Blackwell, Simpson, and Sutherland[7] and Moss and Chasmar[8] reported photoconductivity in PbSe to a wavelength limit of 4 microns when cooled with liquid air, but no photoconductivity at room temperature. Shortly afterwards Starkiewicz[9] successfully prepared the first PbSe cells that were sensitive at room temperature. These cells showed maximum sensitivity at 3.4 microns, followed by a sharp drop at longer wavelengths. In 1949 Moss[10] published similar data. Data taken from their published curves are shown in Fig. 4. Since absolute sensitivities were not reported these curves have been normalized at the long wavelength knee. Although various investigators in the United States have worked on PbSe (notably R. J. Cashman at Northwestern University) no reports of their work have been published in the general literature.

The procedure for preparing sensitive PbSe cells differs rather markedly from investigator to investigator. The shape of the resulting spectral response curve also varies rather widely, but they all show the common property of sharply falling sensitivity beyond 3.3 microns.

This wavelength had been accepted as the "cut-off wavelength" for PbSe. However, in 1951 Gibson, Lawson, and Moss[11] reported the preparation of PbSe cells in which the cut-off wavelength at room temperature was 4.7 microns. No details of

FIG. 3

RESISTIVITY OF PbSe CRYSTALS

DATA BELOW 25° C REPLOTTED FROM BAUER

INTRINSIC LIMIT CALCULATED FROM [$\Delta E = 0.24$ ev; $\mu = 400$; $m_e^* / m_e = 1$]

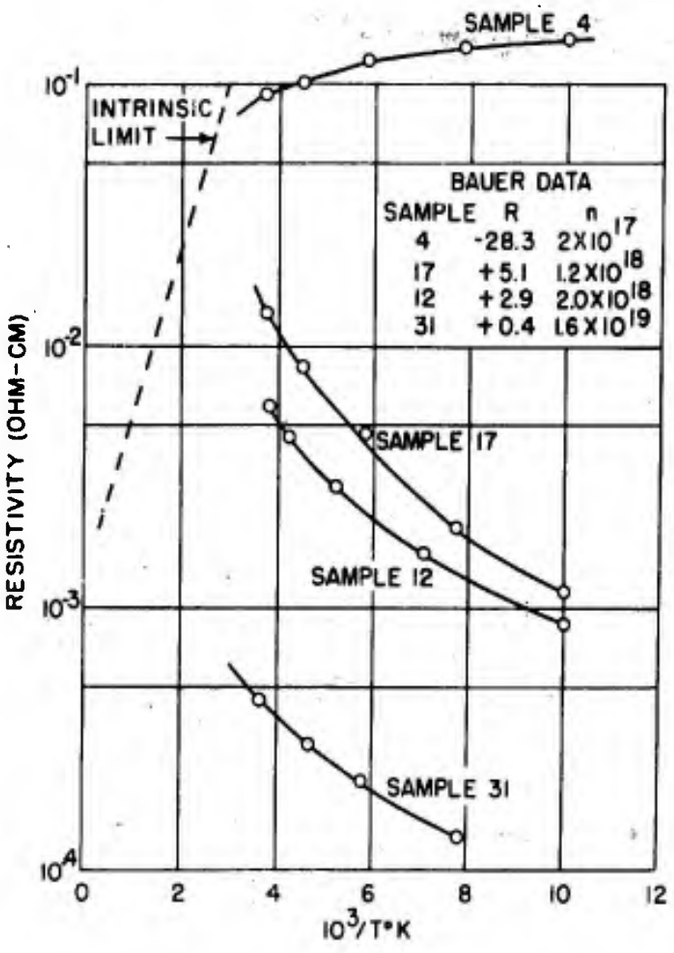

FIG. 4

Pb Se SPECTRAL RESPONSE AT 25°C

OTHER LABORATORIES

NORMALIZED AT LONG WAVELENGTH KNEE

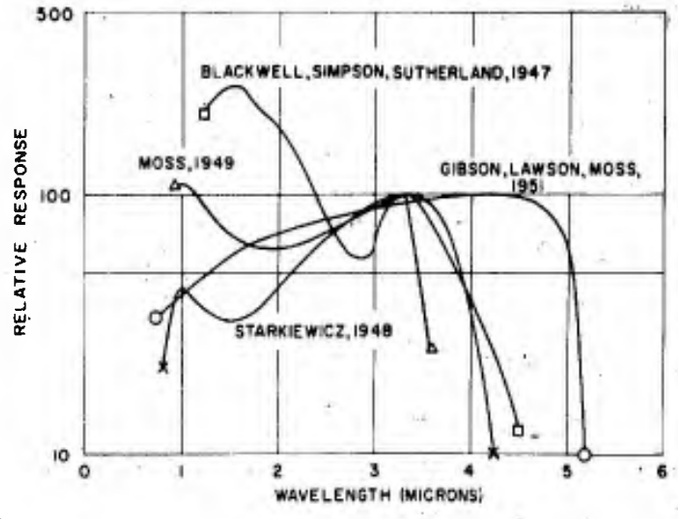

the method of preparation nor absolute sensitivity level were given. It was indicated that tne films showing this behavior were quite thick compared with previous films. Their curve is also included in Fig. 4.

CHAPTER II

THE EXPERIMENT IN BRIEF

SECTION A. Aims and Measurements

The purpose of this work has been to obtain information as to the mechanism of photoconductivity in PbSe. It has been approached through a study of the sensitization procedure. The process of preparing films was varied by the use of starting materials prepared in various ways, by substituting other chemical elements for the known sensitizing agent (oxygen), and by varying film thickness and heat treatment. The range of conditions which produce sensitivity, together with major differences in the type of sensitivity achieved in each case, is then used to develop a model of photoconductivity.

The electrical measurements which have been utilized to evaluate the effects of the sensitizing procedures are the following:

1. Resistance as a function of temperature.

2. Sign of the thermoelectric power. This is a simple method of determining the sign of the predominant current carrier.

3. Time constants of the photoconductive response at high and low temperatures.

4. Relative response to black-body illumination.

5. Spectral variation of response.

SECTION B. Material Requirements

For any study in which the structure and condition of a semiconducting film is concerned we must recognize that impurities introduce energy levels not present in the pure material, which can affect the electrical and optical properties. A deviation from stoichiometric proportions of the component elements will also introduce "impurity levels". Furthermore these proportions may be changed irreversibly by heat treatment. These deviations enter as mechanical defects in the long-range order of the sample. Thus an ion (a Pb^{++} ion or a $Se^{=}$ ion, in this case) may be moved from the body to the surface of the sample, leaving a lattice defect (Schottky defect)[12]. Or such an ion may move into an interstitial position within the crystal, producing two defects, (Frenkel defect)[12]. In films narrow gaps between crystallites may produce surface levels which will create electrical barriers between the crystallites. Because of this last effect single crystals will yield results rather different from those obtained on thin films. (Indeed, some measurements cannot be interpreted except from single crystal data.) We will see these differences particularly in the resistance-temperature data presented below.

CHAPTER III

MATERIALS PREPARATION AND FILM DEPOSITION

SECTION A. Materials Preparation

The need for highly pure materials has been mentioned. A search of the manufacturing literature disclosed that the American Smelting and Refining Company prepares lead which is pure to 1 part in 10^6. This was considered to be adequate purity. No source of selenium of comparable purity was found, however. Fisher & Company "Micro-pure Selenium Powder" was purchased, and preparations for purification by distillation were made.

A spectroscopic examination of the selenium powder was made, using a Baird 3 meter grating spectrograph. This was converted from the normal arrangement for quantitative analysis to an arrangement yielding higher sensitivity to impurity traces. The image of the source was focused directly on the entrance slit instead of on the grating. This effectively gathers more light from the impurity lines, although bright lines are not reproduced quantitatively.

Using this arrangement, it was found that the selenium powder contained easily detectable quantities of copper, magnesium, lead, silicon, silver, and nickel. No impurities were found in the lead.

The equipment used for purifying the selenium is shown in Fig. 5. The initial charge of selenium powder, compressed into pellets to minimize movement of the powder on pump-out, was placed in the tube at the end away from the vacuum pump. In the initial trials a mercury diffusion pump was used. The system was pumped out and baked to about 200°C. Then a local oven was placed over the section containing the selenium, and heated to 250°C, while a second oven, at 200°C, was placed over the next section. With proper care taken to avoid filling the necks between sections by condensed selenium, 65% to 75% of the initial charge was driven into the second section. Holding it at 200°C insured that any remanent sulfur was not collected with the selenium. At this time the first section was sealed off and discarded. This process was repeated twice more, each time discarding 25% to 35% of the selenium. The final result is triply distilled selenium.

A spectroscopic examination of this material showed only very slight traces of copper, of all the original contaminants. In addition, however, strong mercury lines were found, having entered by back-diffusion from the diffusion pump. Accordingly, the process was repeated with fresh materials in a partial atmosphere of pure helium, using only a forepump. This resulted in elimination of the mercury problem as well as removal of the other impurities.

The selenium was found to take either the metallic or the vitreous phase, depending on the annealing process followed. If the selenium is quenched from the liquid state, the vitreous (non-conducting) phase results. If the solid is held at a temperature slightly above 217°C for a time, and slowly cooled, the vitreous material goes over to the crystalline (conducting) phase. Figs. 6a and b show samples of vitreous and crystalline selenium, respectively.

The pure lead and selenium were combined to produce PbSe by mixing equal atomic parts (stoichiometric proportions) of lead chips and selenium crystallites intimately and compressing this mixture into a pellet. This was then placed in a porcelain crucible in a pyrex tube, and the whole assembly placed in an oven at 450°C, under a helium atmosphere. The materials react exothermally. The resulting PbSe is a metallic, gray, porous piece. Fig. 6c shows a portion of such a sample. Other portions were ground in a mortar and stored in glass for later use.

At a later period in this investigation fairly large crystals of PbSe became available, through the efforts of Dr. R. F. Brebrick of the Naval Ordnance Laboratory. He prepared the materials using techniques similar to those described above. Crystals were grown from the lead selenide by a modified Stockbarger or isothermal cooling process. The PbSe is melted, and the temperature of the sample slowly lowered in such a manner that the lower

FIG. 5
APPARATUS FOR PREPARATION OF HIGH PURITY SELENIUM

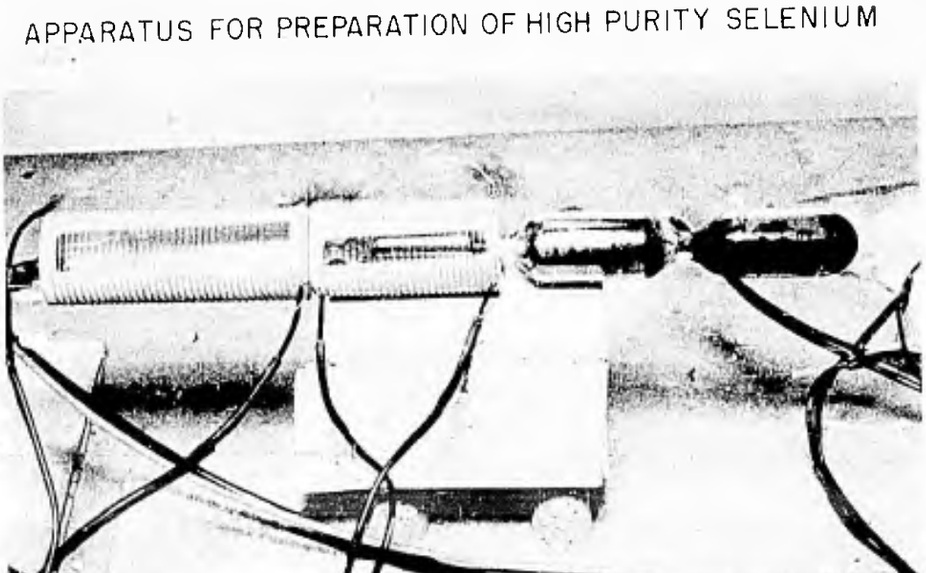

FIG. 6
FORMS OF Se AND PbSe

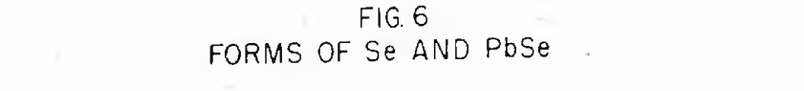

(a) VITREOUS SELENIUM

(b) POLYCRYSTALLINE SELENIUM

(c) POLYCRYSTALLINE PbSe

(d) SINGLE CRYSTAL OF PbSe

(e) PRECIPITATED PbSe

portions were cooler than the upper portions at all times, isotherms being maintained as nearly horizontal as possible. By this technique pure crystals about 1 cm. on an edge were prepared (Fig. 6d).

Subsequently, lead selenide was prepared by the methods of wet chemistry. Hydrogen selenide gas was bubbled through a solution of lead acetate, precipitating lead selenide. The dried precipitate is shown in Fig. 6e.

SECTION B. Cell Construction

In order to study the electrical and photoconductive properties of PbSe, thin films were prepared within evacuated glass cell blanks. Two principal styles of cell were developed: the single-walled or room-temperature cell, and the dewar style, coolable cell. Figs. 7a and 7b are two views of a dewar cell blank. Fig. 7c is a completed dewar cell. Fig. 7d shows two completed single-walled cells. The single-walled cell is far simpler to prepare and simpler to handle than the dewar type. Accordingly, a large percentage of this study utilized this general design. Cells were numbered serially starting with #301 to avoid confusion with another series (Te and PbTe) studied previously in this laboratory.

In the single-walled cell, aquadag (graphite) electrodes were painted onto the inner surface of the thick (concave inward) end of the cell. Tungsten leads, sealed through the glass,

permitted external electrical connections to the aquadag. After the aquadag was painted in place, it was heated to a dull red heat to sinter the carbon particles, thus producing a quiet, low resistance film. At this time a very thin "bubble window" was blown into place. A 1 to 5 micron thick bubble of pyrex or nonex glass, if free of imperfections, may be pumped to a vacuum of 10^{-7} mm. of mercury or better on the convex side, and will maintain itself even at temperatures near 500°C for reasonable lengths of time. This temperature, required for treatment of the PbSe, is near the softening point of nonex so extreme care must be used.

Such a window can be prepared consistently by a skilful glassblower, and is found to transmit infrared to a wavelength of 6.5 microns. Fig. 8 shows the transmission through nonex films of various thicknesses as a function of wavelength. The transmission was measured using a Perkin-Elmer Model 21 double beam infrared spectrometer, and the thickness of the windows was measured interferometrically.

The dewar cell utilizes the same type of electrode and bubble window as used in the single-walled cell. The principal difference encountered in using this type of cell as compared to the single-walled cell (aside from the ease of cooling the film) is the fact that the film is deposited on the outside of the inner member, where it is not so easily available for flame heat treatment. It is also somewhat more difficult to control the deposition.

NAVORD REPORT 3922
FIG. 7
CELL STRUCTURE

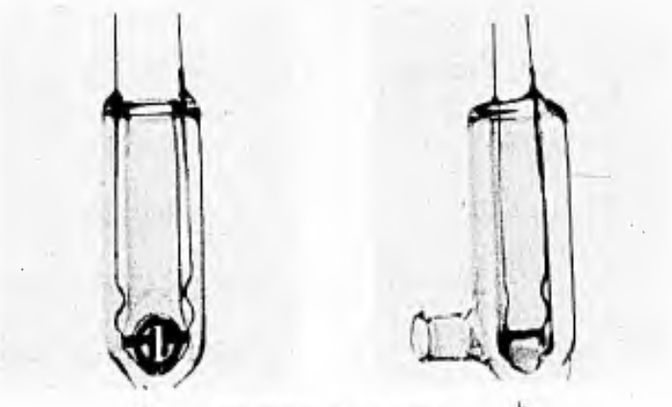

a DEWAR BLANKS b

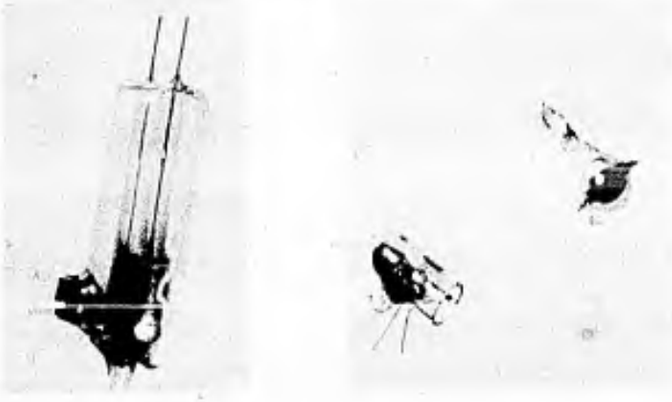

c COMPLETED DEWAR CELL

d COMPLETED SINGLE-WALLED CELLS

FIG. 8
TRANSMISSION OF INFRARED
BY BUBBLE WINDOWS OF VARIOUS THICKNESSES

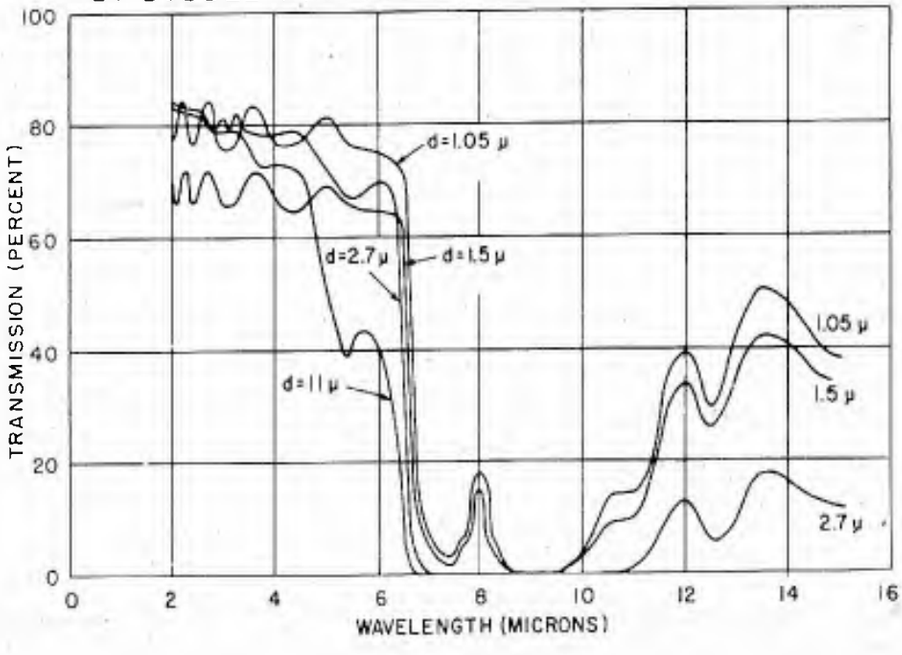

SECTION C. Deposition of PbSe Films

Two vacuum systems were constructed in the course of the investigation. A mercury system using two 2-stage diffusion pumps and a liquid nitrogen cold trap was used originally; it reached a vacuum of 1×10^{-7} mm. of mercury or better rather easily. Because of reports which indicated the possibility of poisoning of the photoconductivity by mercury vapor a second system using a three-stage air-cooled oil diffusion pump was constructed. This system (Fig. 9) was constructed in a form that was not easily baked out. Therefore, it normally operated at a vacuum of somewhat better than 10^{-5} mm. This relatively poor vacuum was shown to yield results consistent with those obtained on the somewhat more cumbersome mercury system.

There are essentially two methods available for collecting a film of PbSe in the area between the aquadag electrodes. In the oven method the whole cell blank containing a small sample ($\sim$1 milligram) of PbSe, either crystal or (preferably) powder, is evacuated and an oven at 450°C-500°C placed around it. A jet of room-temperature air is directed at the area on which the deposit is desired. This area does not include the electrodes, but rather is a surface facing the electrodes.

Depending on the temperature of the oven, the size of the powder particles, the amount to be deposited, and the temperature of the airjet, the deposition may take from 10 to 30 minutes. When sufficient material is gathered, the cell is brought to room

temperature. Then a fairly rapid heating with a hand (gas-air) torch can be used to drive the PbSe across through the cell to the electrodes. If the film produced is not sufficiently thick the whole operation must usually be repeated, allowing a longer time for collection of PbSe. The bubble window must then be carefully torched free of PbSe. This two-stage deposition process has been found to yield quieter cells than can be produced by making the initial collection on the electrodes.

When using single-walled cells either the oven method or the following simpler technique may be used for depositing the PbSe: the sample (ground to a powder) is introduced and the cell evacuated and baked out to 350°C. Then after the cell is cooled, a hand torch is used to evaporate the PbSe powder. Since the whole surface of the cell is available for flaming, the PbSe can be driven successively from surface to surface, gradually collecting a film of the desired thickness between the electrodes. Continuous control of film thickness is thus possible. This method cannot be used with the dewar type cell.

SECTION D. Determination of Film Thickness

In order to determine the approximate thickness of the PbSe films a number of samples were prepared in a manner permitting gravimetric thickness measurements. It was assumed that a rough estimate of the thickness of a particular film within a cell blank could be obtained visually by comparing it (color and

transparency as seen in transmission) with the measured samples. For this purpose a group of 180 mm. x 1/10 mm. glass cover discs were carefully cleaned, dried and weighed. Each disc was placed on a heavy (2 mm. thick) 1" pyrex disc, to prevent warping under heat, and sealed into a pyrex tube with a small quantity of PbSe. The tubes were evacuated and baked. Finally a uniform layer of PbSe was deposited on each disc using a hand torch. A range of thicknesses were prepared. The discs were then reweighed and the diameter measured. Using the bulk density the film thickness was calculated from the increase in weight.

It was found that a range of thicknesses from about 0.1 micron to 1 micron gave transparent to translucent films ranging from medium brown to almost opaque. This range is intermediate among the films considered in the pages to follow. Since the usable limit of accuracy of the balance available corresponded to the 0.1μ thickness, and differences between two films each thicker than the minimum thickness which produces opacity cannot be distinguished by observation, this range represents the maximum available by such a comparison. From this it is estimated that films as thin as 0.01 micron and as thick as 5 microns have been prepared and studied at various times in the course of this investigation.

CHAPTER IV

SENSITIZATION PROCEDURE AND EXPERIMENTAL RESULTS

SECTION A. General Description of Sensitization Procedure

The introduction of sensitizers was carried out by either of two processes. In the first, the desired pressure of the sensitizer was established in the cell, and then the film of PbSe was vaporized one or more times, driving it ultimately onto the electrodes while the pressure was maintained. In the second method, once the "standard initial condition" (see SECTION B) was obtained the PbSe was not re-evaporated. The sensitizer pressure was established, and the cell brought to the desired temperature and held for the appropriate time. Following this the cooling curve could be measured. This latter method was generally used for treatment with sensitizers having low vapor pressures at room temperature. This method was also necessary with the more corrosive gases (Br_2 especially).

In the case of the sensitizers which are gases at 25°C it was generally possible to measure an effective pressure, using a thermocouple gauge or Philips gauge. No attempt was made to convert the readings to absolute values, but the effective pressures were recorded using the gauge calibration for air. Since no numerical calculations were based on the pressure readings the use of effective pressure is permissible.

It was possible to make certain measurements on the cells at each stage of the treatment. Other measurements were possible only when the film showed adequate photosensitivity. The procedure followed in treating a sample was the following:

Starting with a low resistance n-type sample, a cooling curve of resistance was obtained. The cooling rate was usually such that the range from 400°C down to 50°C was covered in about 45 minutes. The temperature was measured by a chromel-alumel thermocouple placed in contact with the outside of the cell envelope as near the sensitive area as possible. Metal baffles were used around the cell to prevent excessive temperature gradients or convection currents.

On completion of the initial cooling curve the cell was isolated from the pumps, using a mercury cut-off (a stop-cock in the case of the mercury-free system), and a small sensitizer pressure was established. The cell was heated to the highest temperature to be used, and held until equilibrium was reached. A new cooling curve was then taken.

At the completion of this and successive cooling curves it might be desired to determine the sign of the carrier, and whether any appreciable photosensitivity had resulted. If one electrode is cooled slightly a thermal emf. will be established. Since the relative thermoelectric power of the semiconductor is usually much greater than that of the aquadag, the sign of the resulting voltage will show the type of current carrier predominating. A

temperature gradient will cause diffusion of the carriers to take place, until the emf. produced is in equilibrium with the excess thermal energy; thus a higher concentration of the predominant carrier will be found at the cold junction. In an n-type sample the cold junction will thus become negative with respect to the warm junction. The cooling may be achieved by the use of a small piece of dry ice. Near the end of a cooling curve it may be more convenient to direct a jet of room-temperature air against one electrode while the other is still warm.

This measurement is reliable except when very near to zero thermal emf. Here a small displacement of the zero in the thermal emf-vs-carrier concentration curve produces a region of error. (However, by using a low-sensitivity potentiometer one can normally not get a readable deflection in this condition since the resistance becomes very high.)

To determine the presence or absence of photosensitivity a 6 watt (110 volt) tungsten bulb is held as close to the sensitive surface as possible. With the dewar-type cell it is placed at the window. With the single-wall construction it is held in contact with the area containing the sensitive surface. The resistance with and without illumination is recorded. The fractional change $\Delta R/R$ is a rough but quick measure of the sensitivity. With this test much lower sensitivities could be detected in the single-walled cells than in the dewar type, because the lamp may be placed much closer to the sensitive area with the single-walled

cells. This fact must be kept in mind when comparing cells of the two types.

When appreciable sensitivity is indicated by this test, a more quantitative test using chopped light from a 500°C black body can be performed. In this test a 10° nichrome Mendenhall wedge is heated electrically. An image of the open face of the wedge is formed on the cell by a concave mirror, after passing through a three-sector light chopper. The resulting square-wave radiation is allowed to fall on the film, which is connected into the circuit of Fig. 10. The signal produced shows the magnitude and time constant of the response. The ac voltage output of the circuit when the shutter is held closed is the current noise of the cell. Sensitivities of two types are of interest: magnitude of signal, and signal-to-noise ratio.

The response time constant of these films can be obtained directly by either of two measurements. In the pulse method the shape of the response to square-wave illumination is observed on an oscilloscope. If normal exponential response is seen the time in microseconds for the signal to decay to 1/e (0.37) of its maximum value is the time constant (τ). In the second method, the magnitude of the response to square-wave illumination is observed as a function of the repetition rate of the square wave (chopping frequency). Again for exponential response the peak signal can be shown to be given by $S = S_o/\sqrt{1+(\omega\tau)^2}$ where S_o is the maximum response for constant (unchopped)

illumination. Thus the response at low repetition rates is constant, while at high frequencies it will begin to fall off, at a rate increasing to a limit of 6 db per octave. At the frequency f_c at which the slope is 3 db per octave the response is 70% of its low-frequency value. This frequency is then $f_c = 1/2\pi\tau$.

One further measurement is possible when the sensitivity as indicated by the preceding tests is sufficiently high--the spectral sensitivity. Rough portable equipment is used as long as the cell is connected to the vacuum system. More precise equipment can be used for final measurements of cells after they are sealed off from the system.

The portable system consists of a type L-235 Gaertner infrared spectrometer with a rock salt prism, and the chopped nichrome source mentioned above. The resolution available is better than 1 micron per millimeter slit width over the whole range. Thus when the cell sensitivity is high enough to use slits 0.1 mm. or narrower the desired minimum resolution of 0.1μ is attained. This equipment is shown in position for use in Fig. 9.

The better monochromator is a Leiss double monochromator using rock salt prisms. The source is a globar operated at 1000°C; the radiation is normally chopped at 90 cps. by a three-sector disc. The resolution for all slit widths used is 0.1μ or better. A block diagram of the set-up used for these measurements is shown in Fig. 11.

FIG. 9
EQUIPMENT FOR PREPARATION AND STUDY OF PHOTOCONDUCTIVE PbSe FILMS

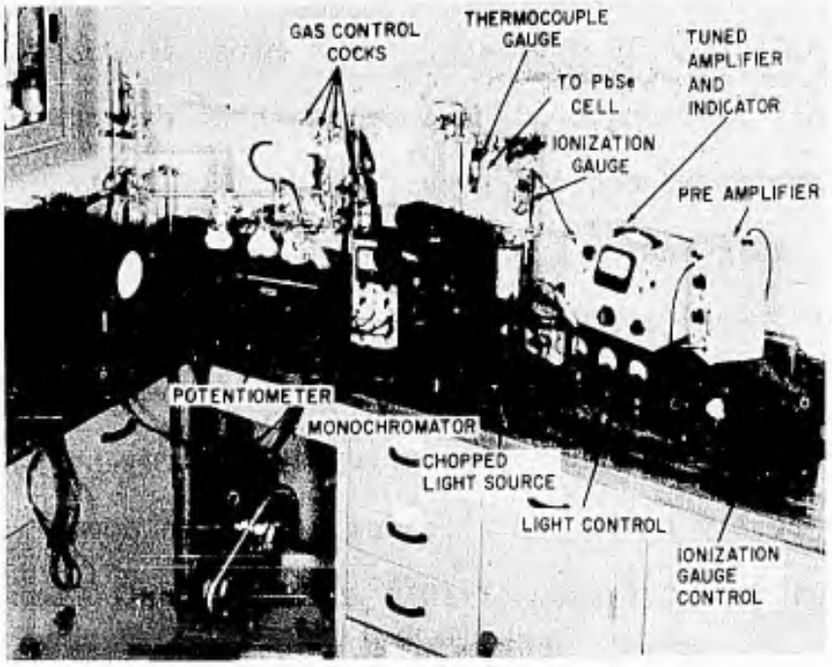

FIG. 10
CIRCUIT DIAGRAM FOR AC RESPONSE

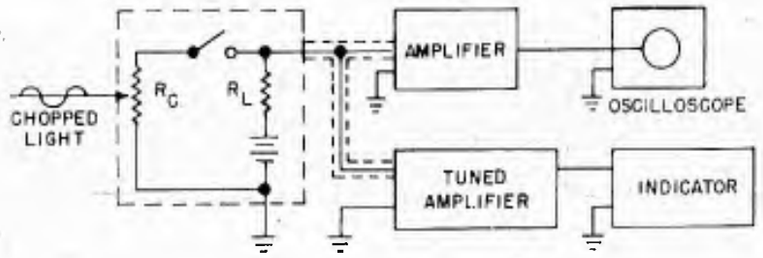

FIG. 11
MEASUREMENT OF SPECTRAL RESPONSE

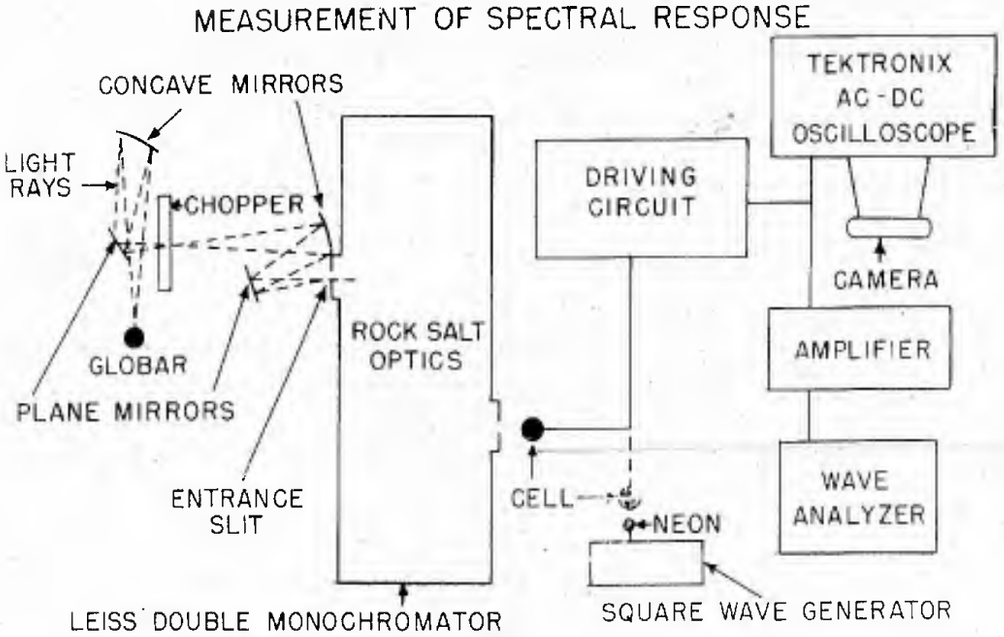

SECTION B. Oxygen Treatment

When a film is prepared as described in CHAPTER III C, its resistance is found to depend on its history and on the temperature at which it was deposited, as well as on its thickness and surface dimensions. It was found, however, that a "standard initial condition" could be obtained reproducibly, by suitable choice of starting materials and heat treatment. Small crystallites freshly cleaved from a crystal of pure, n-type PbSe are used, either freshly ground to a medium to coarse powder, or used as crystallites. A vacuum of 10^{-5} mm. of Hg or better was found to be adequate for processing. A film is deposited by using either the oven or torch method of CHAPTER III C. This film may be either low or high resistance when first deposited. (It normally will not show photoconductivity at this time.) Repeated short bakes under the above vacuum conditions at a temperature of 350°C to 450°C will gradually lower the room temperature resistance. For the films used here a resistance of 100 to 600 ohms normally is found as the limiting value, depending on dimensions. The temperature dependence considered as "standard" is either an essentially constant resistance from 20°C to 400°C, or in some cases a slight positive temperature coefficient of resistance. Curve a of Fig. 12 is such a curve. It should be noted that Fig. 12 and all the experimental curves presented in CHAPTER IV, are representative samples taken from a large number of similar trials.

In this condition the film will be found to be strongly n-type, by the thermoelectric power test. Films produced by the above process were found to yield reproducible resistance temperature curves. Furthermore, they were found to be essentially free from oxygen, at least as far as its effect in producing photoconductivity is concerned. (This statement will be amplified in SECTION B, 1.) This condition also indicates that there are no significant inhomogeneities in the film which could be removed by further annealing. The film contains an excess of lead, either in the form of selenium vacancies or interstitial lead.

Curves b-j of Fig. 12 show the effect of oxygen on a film originally brought into the standard condition. Each curve is obtained by heating the film, establishing the air pressure indicated, and then slowly cooling while maintaining the pressure. It is seen that successive oxygen treatments result in a general increase of the slope of the curve, until some maximum slope is attained. Further oxygen now produces a drop in resistance, except at the highest temperatures, together with a reversal of the sign of thermoelectric power, indicating p-type material. Accordingly, the slope of the low-temperature portion of the curve decreases, even becoming negative for extremely heavy oxidations.

However, the resistance at high temperatures is seen to continue to increase, even after an extreme fall of room-temperature resistance has occurred.

If the process is now reversed and the film repeatedly baked in a good vacuum the resistance changes will reverse their course. Curves k to q of Fig. 12 show the effect of repeated vacuum baking. Note that the curves shown are all p-type; also note that the high-temperature resistance now decreases while the low-temperature resistance increases. The highest curve (q) in this sequence is quite similar to curve (h). Curves (i) and (j) are redrawn.

In order to show the effect of the oxygen on the resistance at a given temperature the data of Fig. 12 have been replotted in Fig. 13. Each curve in Fig. 13 is an isotherm for a temperature T_i, obtained by plotting the pressure maintained for a particular cooling curve (Fig. 12) as abscissa, and the measured resistance at temperature T_i as ordinate. Four representative temperatures through the range have been plotted. We see that at low and medium temperatures the resistance passes through a peak as the pressure (degree of oxidation) is increased, dropping off for high pressures. We also see that the pressure producing the peak resistance is higher for higher temperatures, until at 375°C a maximum is not reached with the pressures used here.

In Fig. 14 similar resistance-temperature results are shown for another cell in which the measurements were extended down to -195°C. In this case oxygen was introduced by 15-second bakes at high temperature, and the cooling curves were taken after pumping the oxygen out. Higher oxygen pressures were thus needed to

FIG. 12
RESISTANCE-TEMPERATURE DATA
AIR TREATMENT

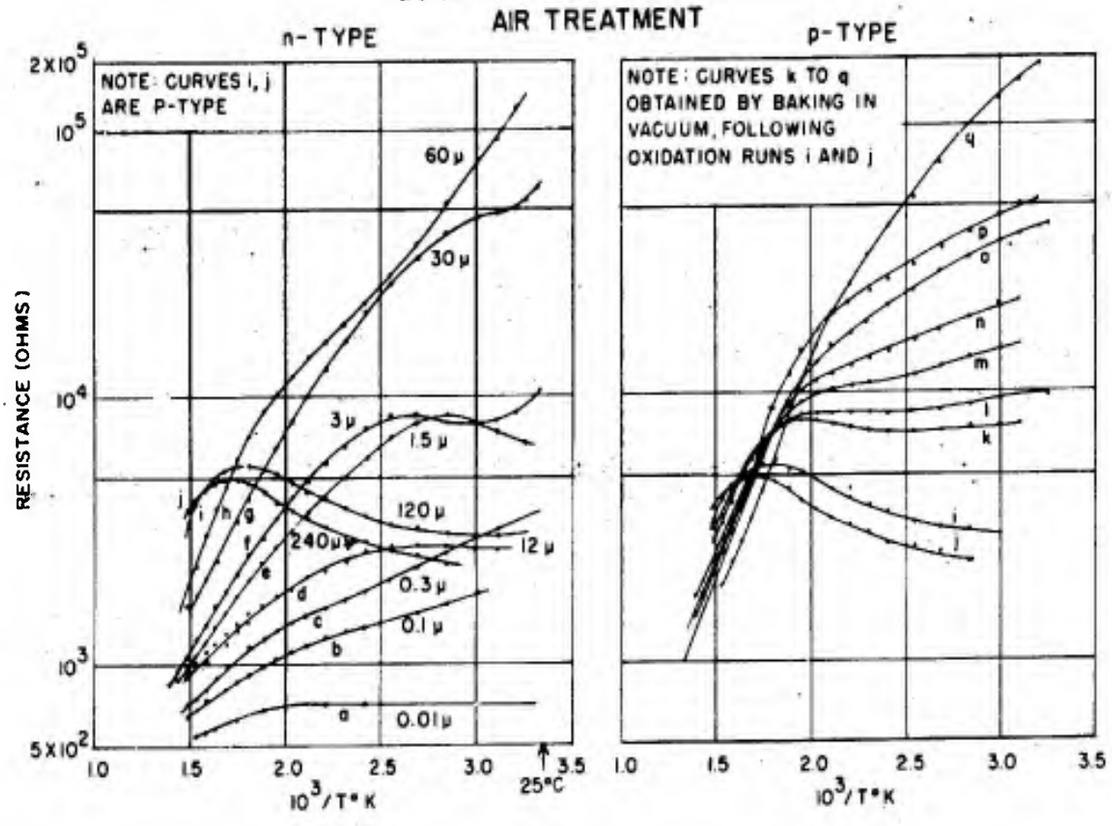

FIG. 13
RESISTANCE-PRESSURE CURVES; AIR TREATMENT

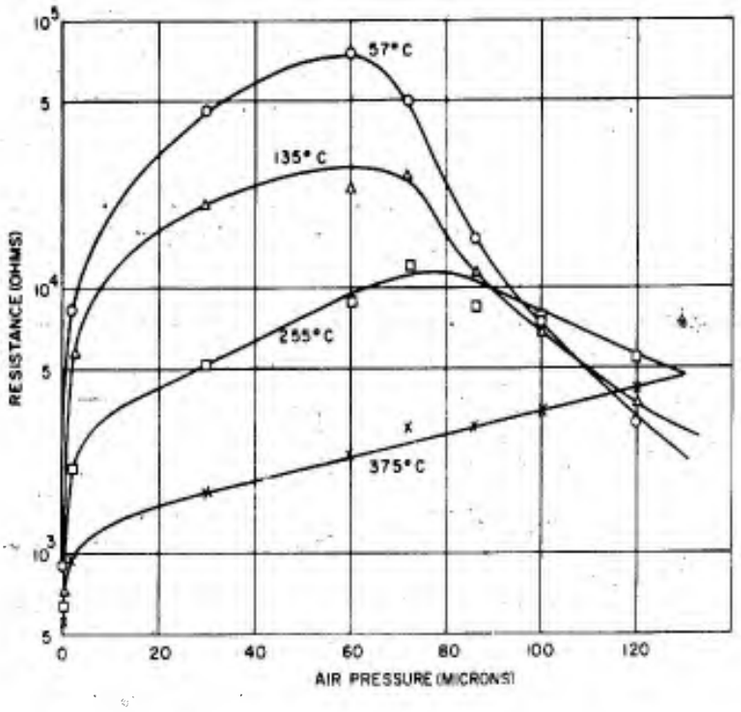

produce a given change as compared to the cooling curves taken under constant oxygen pressure.

If the sensitivity of the film is checked after each heat treatment, using the methods described in SECTION A, it is found that the highest sensitivity is achieved only near the condition of maximum resistance, which is the condition where the sign of the carrier is found to reverse.

Fig. 15 shows the results obtained for the spectral sensitivity of various cells at room temperature, taken with the Leiss monochromator. Note that two rather different limiting responses at long wavelengths are found. If one defines the limit in terms of the position of the knee, a value of 3.3 microns is found for cells 388 and 396 and about 4 microns for cell 311. Because of its low sensitivity no knee is defined for cell 313. Even so the data show that this cell response is relatively flat well beyond the region of constant response of cells 388 and 396, not showing the steep drop characteristic of a long wavelength limit. Cells 388 and 396 are thin films, estimated to be 0.1 and 0.5 microns thick respectively. Cell 311 is a very thick film, thickness probably between 2 and 5 microns. Cell 313 is a film of moderate thickness, about 1 micron thick. It is a low resistance n-type film, probably not sensitized sufficiently to reach the condition of maximum sensitivity.

When a cell is cooled to -195°C it may show either the normal type of response seen at room temperature, with immediate

recovery to the original dark resistance when the light is removed, or a "frozen-in photoconductivity" in which the resistance does not recover when the light is removed. In this case if the cell is warmed to room temperature and then recooled, the original dark resistance will again be attained. Frequently a partial recovery will occur when the light is removed, indicating that two separate processes can occur either independently or together.

Fig. 16 shows the spectral response of several dewar-type cells operated at liquid nitrogen temperature; only the fast recovery component is included, since ac methods were used. The curves are adjusted to a common level (S/N =10) at 6 microns, to simplify comparison of the various long-wavelength limits. Again we notice a variation in position of the knee. Cell 444, a transparent film, has a knee at 5μ. In contrast, the thicker films 311 and 313 have a minor knee near 5μ with a sharp knee near 6μ. The response of cell 444 has dropped by a factor of 30 before cell 313 changes significantly.

Although the correlation is not complete, we see in these two plates that the region of constant response for thick films extends to longer wavelengths than it does for thin films; no changes in processing procedure were made for thin films as compared to thick films.

The time constants of all cells whose response is shown in Fig. 15 were too short at room temperature to be measured with

FIG. 14
RESISTANCE-TEMPERATURE DATA
AIR TREATMENT
15 SECOND BAKE AT 400°C AT PRESSURE P

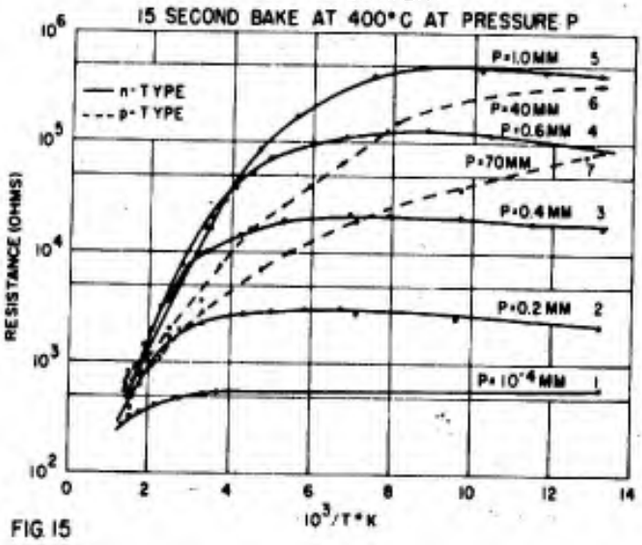

FIG. 15
SPECTRAL RESPONSE AT 25° C...
AIR-SENSITIZED FILMS

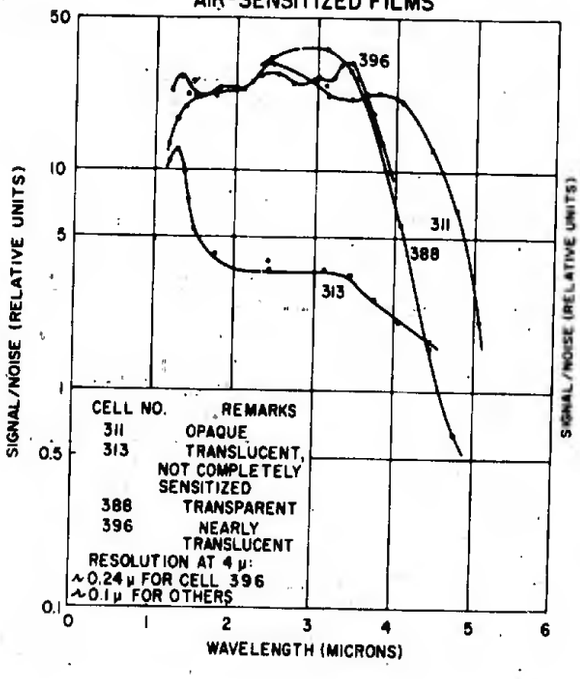

FIG. 16
SPECTRAL RESPONSE AT -195° C
AIR SENSITIZED FILMS
(CURVES NORMALIZED AT 6 MICRONS)

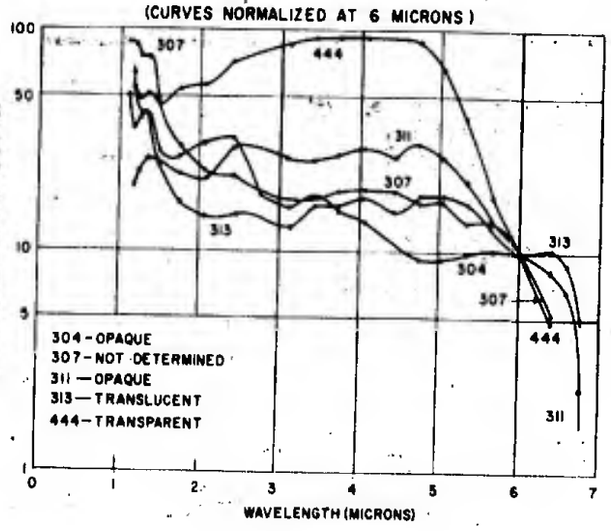

equipment available at this time. It has been the experience of all other investigators that these time constants range from 5 microseconds down to less than 1 microsecond. Fig. 17 shows the wave-form observed using square-wave chopped light (chopping frequency 90 and 900 cps.). Fig. 17a is the response at 25°C of cell 311 to 90 cps. chopping; it is typical of all cells observed at this temperature. The response at 900 cps. is not observably different. At reduced temperature, however, the time constant becomes longer. For an n-type film at -195°C time constants (measured as described below, using Eq. 3) from 15 to 40 microseconds are found; for a strongly p-type film the time constant is of the order of 5 milliseconds. Fig. 17b shows the response at -195°C to 90 cps. chopping for a nearly stoichiometric cell, (#311). The same cell begins to show some curvature when 900 cps. chopping is used, as shown in Fig. 17c.

Fig. 17d is a strongly p-type film at -195°C. The chopping frequency is 90 cycles; the time constant is seen to be of the order of 5 milliseconds.

In Fig. 17e we see the more general case of a cell showing both types of response simultaneously at -195°C. This cell is nearly stoichiometric.

Sometimes it is found that a cell shows a very fast response at 25°C and at -195°C, as in 17a and 17b, and two time constants at intermediate temperatures. A typical example at -78°C is seen in 17f.

If the amplitude of response is observed as a function of chopping frequency, a cell possessing only one time constant will obey the relation

$$\Delta n = \frac{aI\tau}{[1+(\omega\tau)^2]^{1/2}} \qquad (3)$$

(see Eq. A3). This yields a response which is essentially flat at low frequencies, where $\omega\tau < 0.25$; at higher frequencies the response falls off slowly at first but increasingly fast until a limiting rate of 6 db per octave is achieved. At the frequency yielding $\omega\tau = 1$ the slope is 3 db per octave and the magnitude is down 3 db (to 70% of the low-frequency value). By determining the frequency at which this occurs the numerical value of the time constant can be obtained. Such a plot is shown in Fig. 18 for cell 311. The time constant indicated is 30 microseconds.

For a cell in which two time constants occur, Lummis and Scanlon[13] have shown that satisfactory estimates of the time constants can be found from the frequency response curve by fitting the data to the approximate equation

$$\Delta n = \left[\frac{A}{[1+(\omega\tau_1)^2]^{1/2}} + \frac{B}{[1+(\omega\tau_2)^2]^{1/2}}\right] \qquad (4)$$

where A and B are relative strengths of the two independent exponentials having time constants τ_1 and τ_2 respectively. Their calculations were compared with the values obtained by analyzing oscillographs of square-wave decay curves similar to those in Figs. 17e and 17f.

FIG. 17 ~
SQUARE-WAVE RESPONSE CHARACTERISTICS OF PbSe

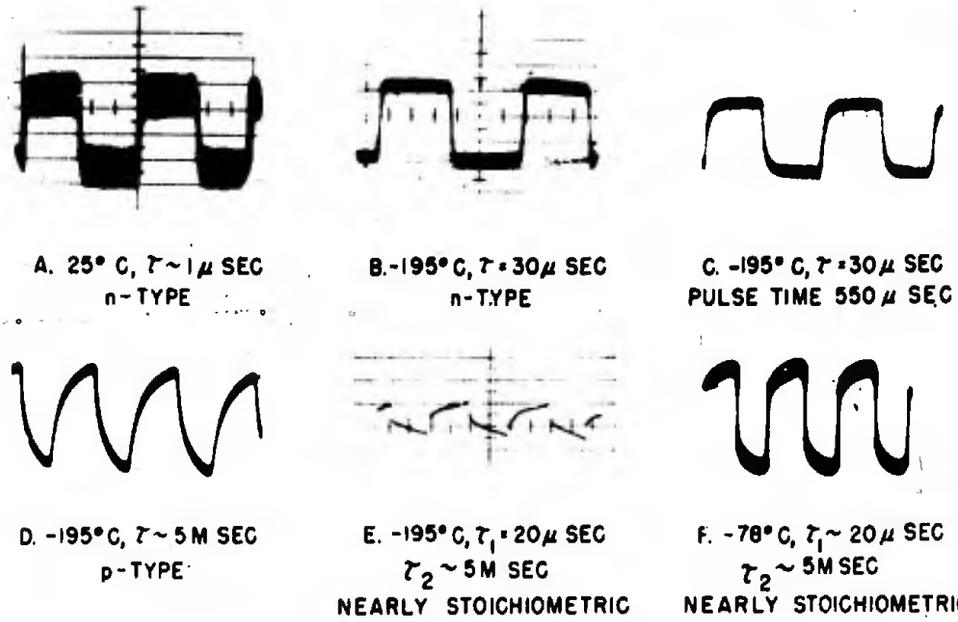

A. 25° C, $\tau \sim 1\mu$ SEC n-TYPE

B. -195° C, $\tau = 30\mu$ SEC n-TYPE

C. -195° C, $\tau = 30\mu$ SEC PULSE TIME 550 μ SEC

D. -195° C, $\tau \sim 5$ M SEC p-TYPE

E. -195° C, $\tau_1 = 20\mu$ SEC $\tau_2 \sim 5$ M SEC NEARLY STOICHIOMETRIC

F. -78° C, $\tau_1 \sim 20\mu$ SEC $\tau_2 \sim 5$ M SEC NEARLY STOICHIOMETRIC

PULSE-TIME = 5.5 M SEC EXCEPT C

FIG. 18
FREQUENCY RESPONSE AT -195°C

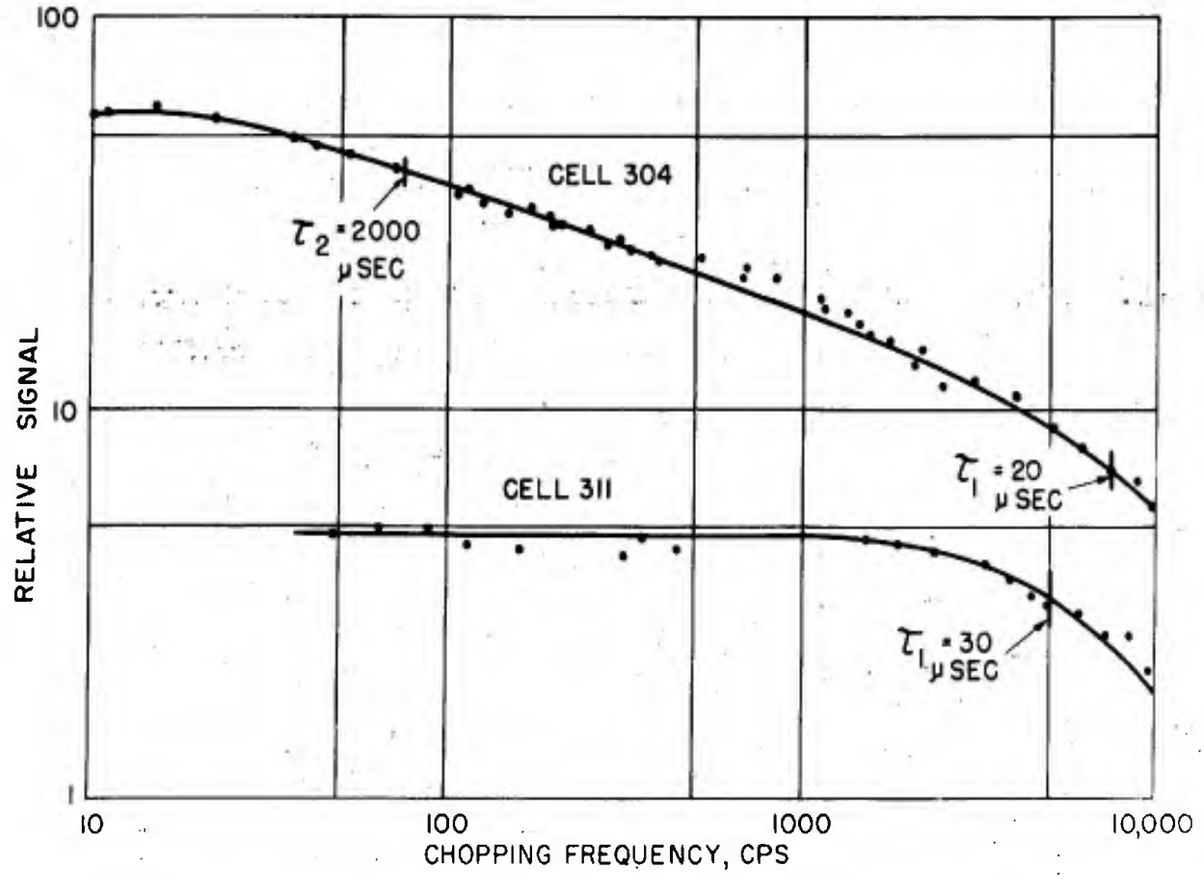

The frequency response curve for cell 304 at -195°C is also shown in Fig. 18. From this curve rough estimates of $\tau_1 \sim 20$ microseconds and $\tau_2 \sim 2000$ microseconds are obtained, as compared to the values $\tau_1 < 50$ microseconds and $\tau_2 \sim 5000$ microseconds estimated from the square-wave response curve in Fig. 17e. Neither of these pairs of values were obtained by precise numerical fitting.

In general it is found that the magnitude of the sensitivity is increased as the cell is cooled from room temperature to -195°C. Many cells show no sensitivity at all at 25°C, but are quite sensitive at -78°C and -195°C. Some exceptional cases show a maximum sensitivity together with a double time constant at intermediate temperatures; in such cases it is possible for the sensitivity at 25°C to equal that at -195°C.

If one plots responsivity (volts of signal per watt/cm^2 of incident radiation) instead of S/N for the thickest and thinnest films, at room temperature, the curves of Fig. 19 result. Here it is seen that the shift of the long-wavelength knee with thicker films is achieved at the expense of responsivity to an extent that no significant improvement is achieved at any wavelength. All attempts to raise the level of response were unsuccessful. This fact will be treated theoretically in CHAPTER VII, where it will be shown that no such improvement should be expected to result merely from the use of thicker films.

1. Processing Parameters

In the process of obtaining the measurements reported in the preceding section PbSe prepared in various ways was studied. The first PbSe used was prepared by direct reaction of lead and selenium, as described in CHAPTER III, and then ground to a powder and stored in glass. This material was used successfully in studying oxygen sensitization over a period of about a year, during which time it was possible to obtain reproducible resistance-temperature data by using the "standard initial conditions". As the study of other sensitizers (see the following sections of this chapter) progressed, however, it became more and more difficult to achieve the low-resistance n-type condition. At this time the single crystals of PbSe became available; this material could be brought into the standard condition with comparative ease. However, it was considerably easier to produce photosensitivity with the powdered material than with the fresh crystals. These facts were interpreted as showing that atmospheric oxygen had slowly diffused into the PbSe and could not be removed by baking. Because of this interpretation freshly ground crystals were used in all subsequent experiments with sensitizers other than oxygen.

Lead selenide produced by wet precipitation was also tested. It, like the powdered material described above, could not be brought into the standard initial condition, and could also be sensitized, using oxygen, with less difficulty than the single-

crystal material. X-ray diffraction powder patterns of all three materials were made by Miss Selma Greenwald, of the Naval Ordnance Laboratory. Two differences were found among the materials; the precipitated material was found to have much smaller crystals, and to contain lines of lead basic acetate Pb(OH) (CH_3COO). Tests with the basic acetate showed that it decomposes under torching and does not deposit with the film. Its effect as a sensitizer was deemed negligible. No significant differences could be observed between the two samples prepared by fusion.

The facts are interpreted to show that the water used to prepare the PbSe contained dissolved air, which became entrapped in the crystals together with the lead basic acetate. The oxygen then acts as a sensitizer just as in the preceding case.

The possibility of mercury poisoning of the films was mentioned as the reason for constructing a mercury-free vacuum system. Although it was found that higher oxygen pressures were required in order to achieve the high resistance condition and photoconductivity when mercury is present, no difference in ultimate sensitivity was detected between the two systems. The mercury thus is seen to retard but not prevent oxidation.

SECTION C. Selenium Treatment

As shown by Hintenberger[5], it is possible to modify the resistance of a PbS film by treatment with sulfur vapor, in a manner analogous to that seen in the oxygen experiments. The

same situation should be true for PbSe and selenium vapor. Moreover, if the sensitivity is produced merely by the process of obtaining high dark resistance (as by reducing the number of free carriers to a minimum) it should be possible to produce sensitivity by selenium treatment.

PbSe films were prepared as described in SECTION B to obtain the standard initial condition (low resistance n-type films). A small quantity of selenium in a side arm was kept in liquid nitrogen during the preparation. Then the nitrogen was removed and the selenium vaporized with a torch, until a small quantity of selenium entered the cell. The resistance and sensitivity to white light were checked at room temperature and liquid nitrogen temperature. Then more selenium was introduced.

The results are shown in Fig. 20. A large change of resistance with added selenium through a maximum corresponding to the position of the thermoelectric null is found at all temperatures. No photoconductivity was found at room temperature at any stage of the treatment with selenium. At liquid nitrogen temperature the white light illumination produced changes of 100 to 1 in the resistance, for high-resistance cases. This was a very rapid response; the "frozen-in photoconductivity" seen in p-type oxygen-treated films was also seen after the 6th and 7th selenium vapor addition. Spectral sensitivity was not measured.

SECTION D. Sulfur Treatment

Since selenium by itself does not produce sensitivity at room temperature but oxygen does, it is of interest to determine whether the element intermediate between them in the periodic table (sulfur) can produce sensitivity. The same procedure was followed as with selenium. Fig. 21 shows the effect on resistance over the range from -195°C to 400°C. Again, the resistance increases to a maximum and ultimately decreases as more and more sulfur is added. No sensitivity is observed at room temperature. At -195°C rather good sensitivity is obtained, including a large amount of the frozen-in photoconductivity. Fig. 22 includes the spectral sensitivity of two such samples, one (442) quite thin (<0.1 microns), the other somewhat thicker (~0.2 microns).

SECTION E. Halogen Treatment

As we have seen in the preceding sections, oxygen seems to be significantly different from sulfur and selenium in that it alone produces room temperature photoconductivity. Many possible reasons for this difference have been considered, including ion size, chemical activity, and possible complex compound formation. Fluorine and chlorine are both active "oxidizing agents", highly electronegative. In addition, iodine is known (Henish)[14] to be an impurity important to selenium rectifiers. Thus it was believed possible that some or all of the halogens might produce photosensitivity. A study of the effect of the halogens in

FIG. 19
EFFECT OF FILM THICKNESS
ON RESPONSIVITY

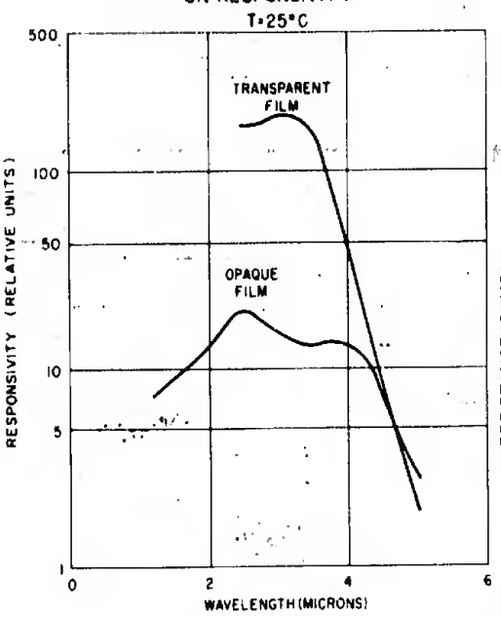

FIG 20
RESISTANCE AT 25° C AND -195° C
EFFECT OF SELENIUM TREATMENT

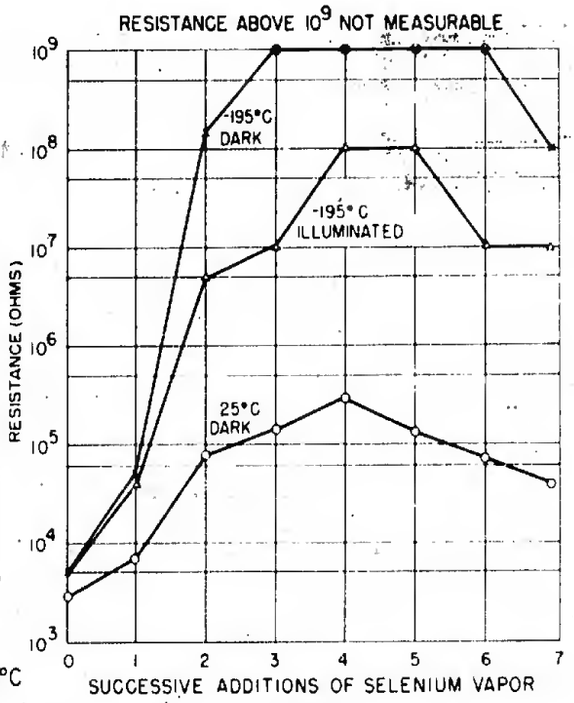

FIG. 21
RESISTANCE AT 400° C, 25° C AND -195°C
EFFECT OF SULFUR TREATMENT

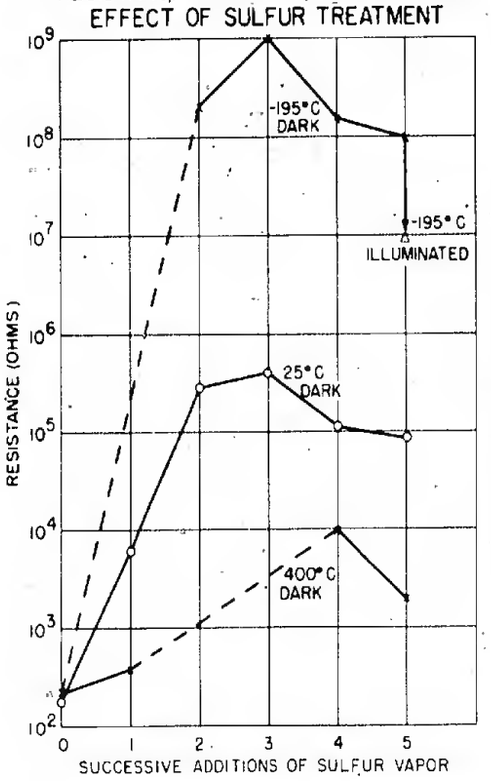

FIG. 22
SPECTRAL RESPONSE AT -195° C,
SULFUR AND FLUORINE SENSITIZED FILMS
CURVES NORMALIZED AT 6 MICRONS
413-FLUORINE; 420-SULFUR; 442-SULFUR
ALL FILMS TRANSPARENT

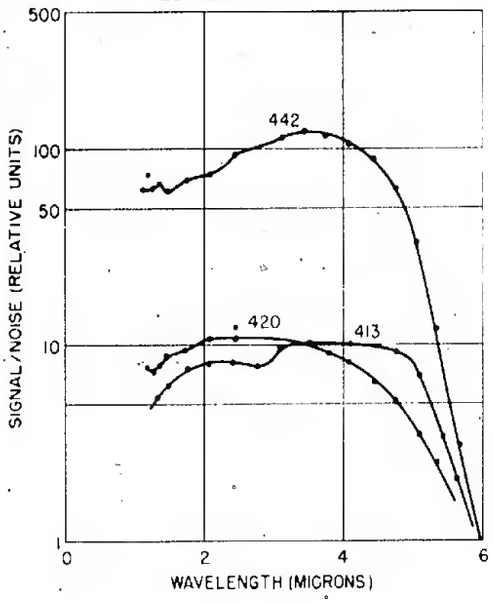

PbSe should serve to reduce the number of possible explanations of the role of oxygen as a sensitizer.

Fluorine was obtained in a form which could be handled easily by the use of CoF_3 powder. This decomposes readily yielding fluorine gas and CoF_2 (solid). At room temperature a fluorine pressure of about 1 millimeter of mercury is found above the CoF_3 so no heating is actually needed. Chlorine gas (bottled) and bromine vapor were used. The initial control of pressure for fluorine and bromine was effected by cooling the supply with liquid nitrogen, dry ice, or cooled alcohol. Iodine was handled in a similar fashion, but with more difficulty because of its lower vapor pressure. Pressure readings were not attempted with the iodine.

Considerable difficulty was encountered in the study of the halogens (particularly chlorine) because of its chemical reaction with stop-cock grease, releasing HCl and CO_2. Difficulty was encountered with "Lubriseal" grease, normally used because of its ability to hold a vacuum to 10^{-8} mm. of mercury or better. Dow-Corning silicone "high vacuum grease" was somewhat more satisfactory chemically, but not completely free from reaction. Finally, Fluorolube grease was obtained* and found to be acceptable, although it is much less satisfactory from the standpoint of vacuum reliability and ease of operation.

*Hooker Electrochemical Co., Niagara Falls, New York

Fluorolube grease is a mixture of polymers of trifluorovinyl chloride, stabilized by replacement of terminal chlorine by fluorine. No hydrogen is contained in the grease. Thus, it is chemically inert. Its composition as a mixture of polymers of various molecular weights is doubtlessly responsible for some of the mechanical difficulties introduced by its use. It was found, for example, that stopcocks appear to become "dry" after a week or so of operation. This was found to be due to the squeezing out of the low-viscosity components from the grease. Light flaming reduced the viscosity of the remaining components sufficiently to permit operation of the stopcock. However, a tendency to leak had to be watched carefully under such conditions.

Figs. 23 and 24 give the dependence of resistance on temperature for various chlorine and fluorine treatments respectively. Note that for small amounts of halogen the curves are very similar to those for oxygen treatment, Fig. 12. A change from n-type to p-type conductivity occurs when the film resistance at room temperature is near its maximum. With heavier treatments a dip in the resistance-temperature curve develops, together with a large positive slope near room temperature.

One of the p-type curves (#8) for chlorine and two (#6 and #7) for fluorine were obtained by pumping on a heavily treated film at high temperature, rather than by continuing the step-by-step addition of the halogen. The value of this procedure is that it verifies that the continued increase at high temperatures is not

due to decreased film thickness. In Fig. 25 the resistance-pressure isotherms for chlorine are presented, obtained from Fig. 23 and plotted just as in the case of oxygen (Fig. 13). Because of the pumping procedure followed, the pressure plotted as 400μ does not correspond exactly to the sequence of increasing pressures. This fact does not alter the qualitative implications of the graph.

An attempt was made to treat a thick (opaque) film with fluorine. It was found that the resistance could not be increased significantly in this case, even by baking under a fluorine atmosphere. This is in contrast to the case of oxygen, where a thick film could be changed in the same way as a thin film.

In the case of bromine it was not possible to get reproducible curves at high temperatures. The bromine was found to attack the film much more severely than either chlorine or fluorine. This is believed to be consistent with the idea of tight binding in the F_2 and Cl_2 molecules: even at the temperatures used here not much decomposition to Cl and F results. Hence, strong corrosive action on the film did not result with these gases.

Fig. 26 shows cooling curves obtained with bromine for pressures sufficiently low that the film was not destroyed. More useful results were obtained at room temperatures, or with quite short heat treatments. Fig. 27 shows the effect of successive additions of bromine at room temperature and at 400°C. A change to p-type conductivity again accompanies the decreased resistance

FIG. 23
RESISTANCE-TEMPERATURE DATA
EFFECT OF CHLORINE TREATMENT

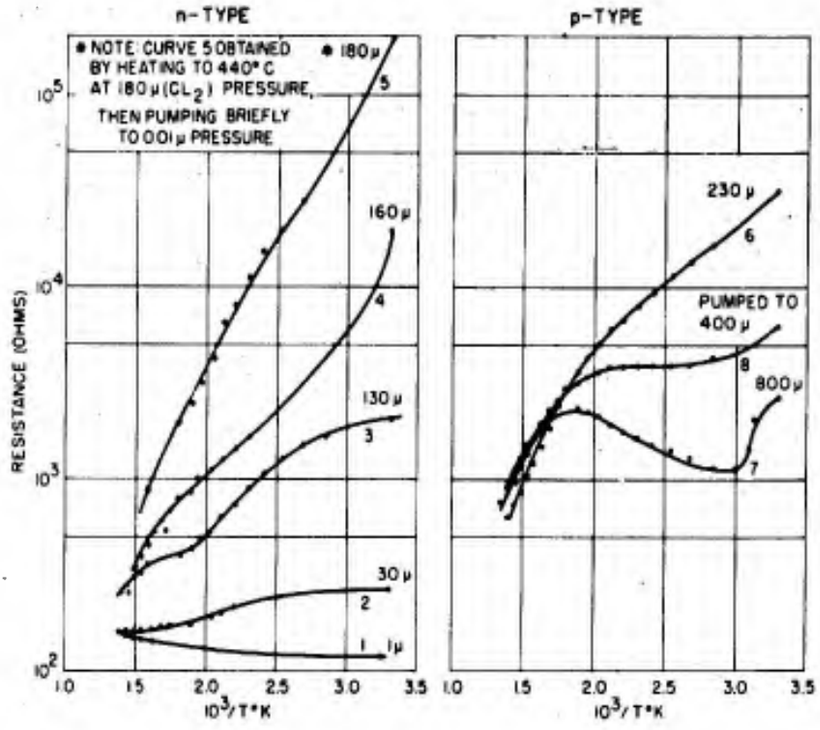

FIG 24
RESISTANCE-TEMPERATURE DATA
FLUORINE TREATMENT

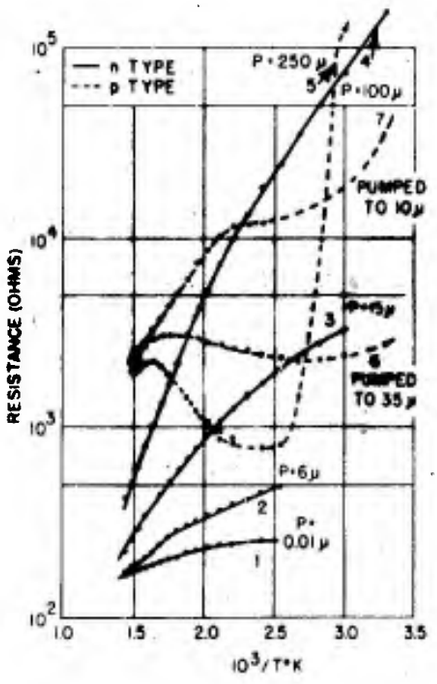

FIG. 25
RESISTANCE-PRESSURE CURVES
CHLORINE TREATMENT

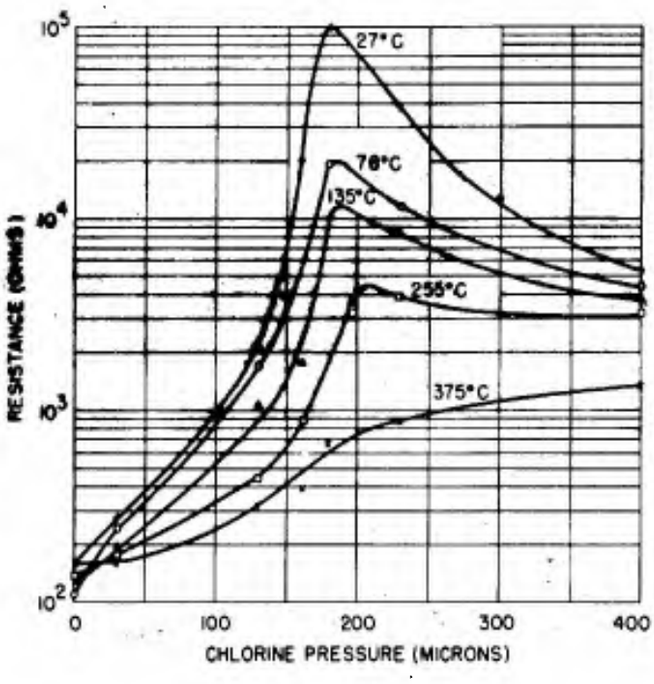

beyond the maximum. Fig. 28, the corresponding curve for the case of iodine additions, is similar to that for bromine.

In the case of each of the halogens, when adequate care was taken to exclude oxygen no photosensitivity at room temperature was found, in spite of the fact that the peak resistance in each case was essentially equal to that produced by oxygen in a film of comparable dimensions. However, if the film was first oxidized until photosensitivity occurred, then baked in vacuum until the "standard initial conditions" of SECTION B were apparently restored, and finally the treatment repeated with the pure halogen, photosensitivity was found to occur at or near the resistance maximum. This photoconductivity shows essentially the same properties as that produced with oxygen alone as regards magnitude, time constant, and spectral limit. Spectral response curves for two cells treated with air and bromine, and one each treated with air and fluorine, air and chlorine, and air and iodine are shown in Fig. 29. The time constant was found to be too short to affect the wave forms of 15 microsecond pulses in a typical cell treated with Br_2 at 250°C. Except for the very insensitive cell treated with iodine the long wavelength knee is seen at 3.3 microns in each case. Because of the wide slits and correspondingly poor resolution used with iodine, no knee is seen in that case. The fluorine-sensitized cell (392) shows a strong increase of sensitivity at short wavelengths. This tendency was noted with all the halogens to a limited extent.

FIG. 26
RESISTANCE-TEMPERATURE DATA

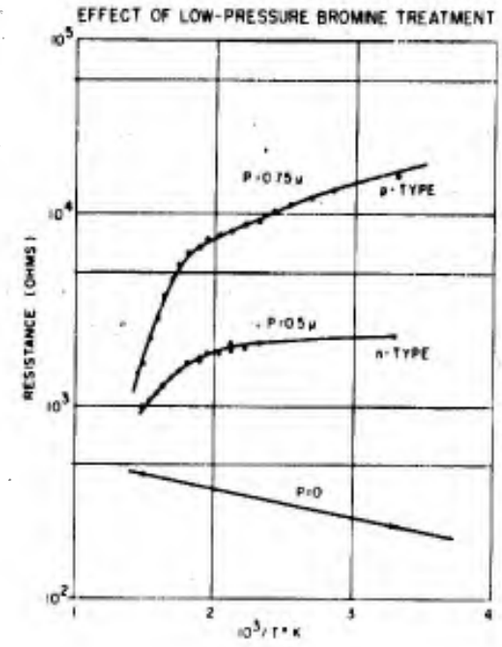

FIG. 27
EFFECT OF BROMINE TREATMENT
ON RESISTANCE

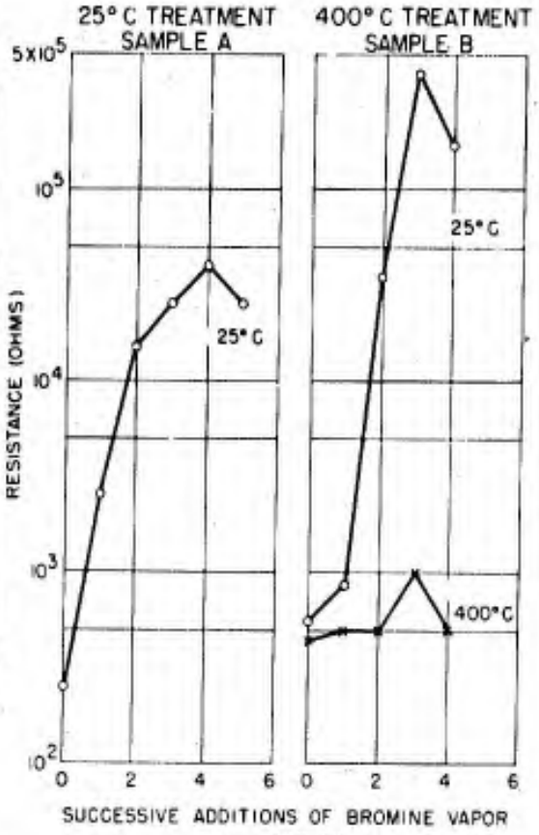

FIG 28
RESISTANCE AT 25° C
EFFECT OF IODINE TREATMENT

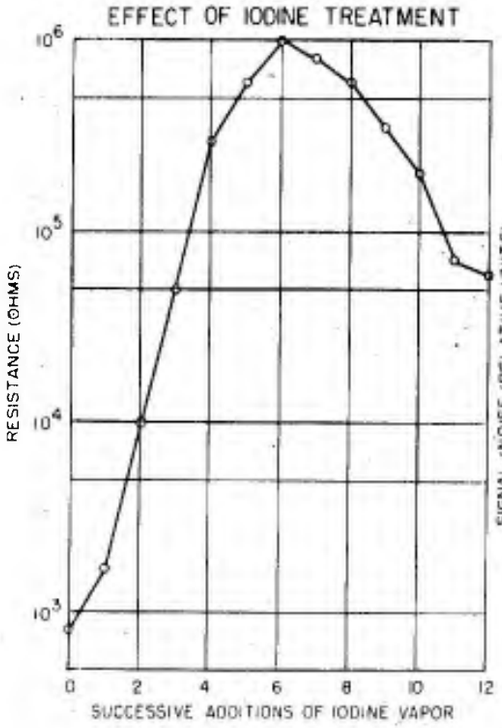

FIG 29
SPECTRAL RESPONSE AT 25° C
HALOGEN SENSITIZERS WITH AIR PRETREATMENT

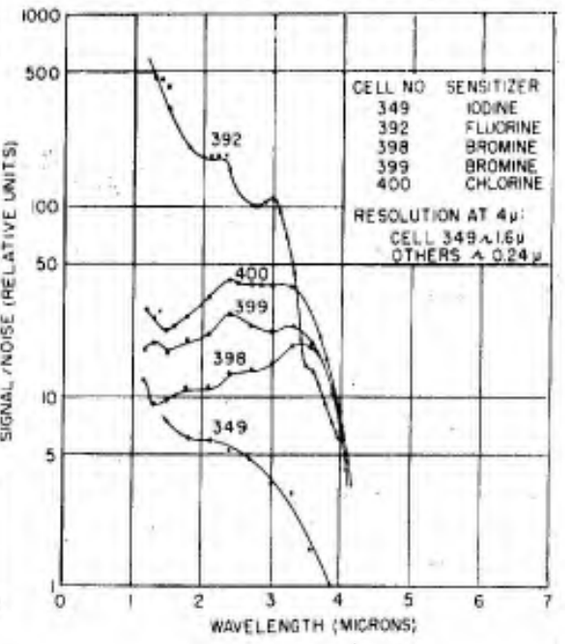

As in the case of sulfur and selenium, photosensitivity at liquid nitrogen temperature was found for fluorine in the absence of oxygen. The spectral sensitivity is given in Fig. 22. Time constants observed were comparable to the fast and very slow response of sulfur and selenium sensitization. No spectral response data was taken at this temperature for the other halogens.

CHAPTER V

INTERPRETATION OF EXPERIMENTAL RESULTS AND FORMULATION OF A MODEL

SECTION A. Basic Mechanisms Involved in Photoconductivity

There are three processes which must be considered in developing a model explaining photoconductivity: absorption of light, release of carriers, and recombination. The first two of these processes have been the central points of difference among theories proposed for the lead sulfide group in the past.

As shown in Figs. 1c and 1d there are two principal absorption mechanisms: main band and impurity absorption. With either mechanism the corresponding energy gap controls the long wavelength limit beyond which photoconductivity cannot arise, while the magnitude of the absorption coefficient at a given wavelength will control the number of free carriers produced per unit light intensity.

In 1950 Gibson[15] reported absorption data obtained from thin films, in which a strong peak occurred around 1 micron, together with a long plateau extending to the limit of his measurement. His curves are reproduced in Fig. 30. He identified the 1 micron peak with the main band transition and the plateau with impurity absorption. According to this the band gaps for PbS, PbSe, and

PbTe at 27°C are 1.2 ev, 0.5 ev, and 0.6 ev respectively. In 1951 Putley and Arthur[16] reported Hall effect measurements supporting this interpretation, giving $\Delta E = 1.2$ ev for PbS.

In 1952 Gibson[17] published crystal absorption data showing an absorption edge at 3μ, 4μ, and 5μ for PbS, PbTe, and PbSe respectively; this edge was believed to be due to impurity absorption.

In 1953 Scanlon[18] showed that the value of 1.2 ev for ΔE in PbS previously obtained by Hall effect measurements was in error, due to irreversible changes occuring during the earlier measurements. He found the band gap to be 0.37 ev, corresponding to the 3 micron absorption edge and to the observed long wavelength limit of photoconductivity. By analogy the main band absorption edge in PbSe would be the one observed at 5 microns, yielding a value of 0.24 ev for ΔE in PbSe. We thus believe the absorption to take place within the crystallites by the mechanism of elevating an electron across the forbidden gap, creating an electron-hole pair. In 1954 Avery[19] published curves for the extinction coefficient calculated from reflectivity measurements made on crystals of PbS, PbSe, and PbTe. These data showed high absorption up to an edge occurring at about 5 microns, in PbSe, essentially in agreement with Scanlon's and Gibson's data.

The second process, release of a carrier, is the current principal target of many investigators. We can identify two points of view, the "numbers theory" and the "barrier modulation

FIG. 30
ABSORPTION IN THIN FILMS
GIBSON

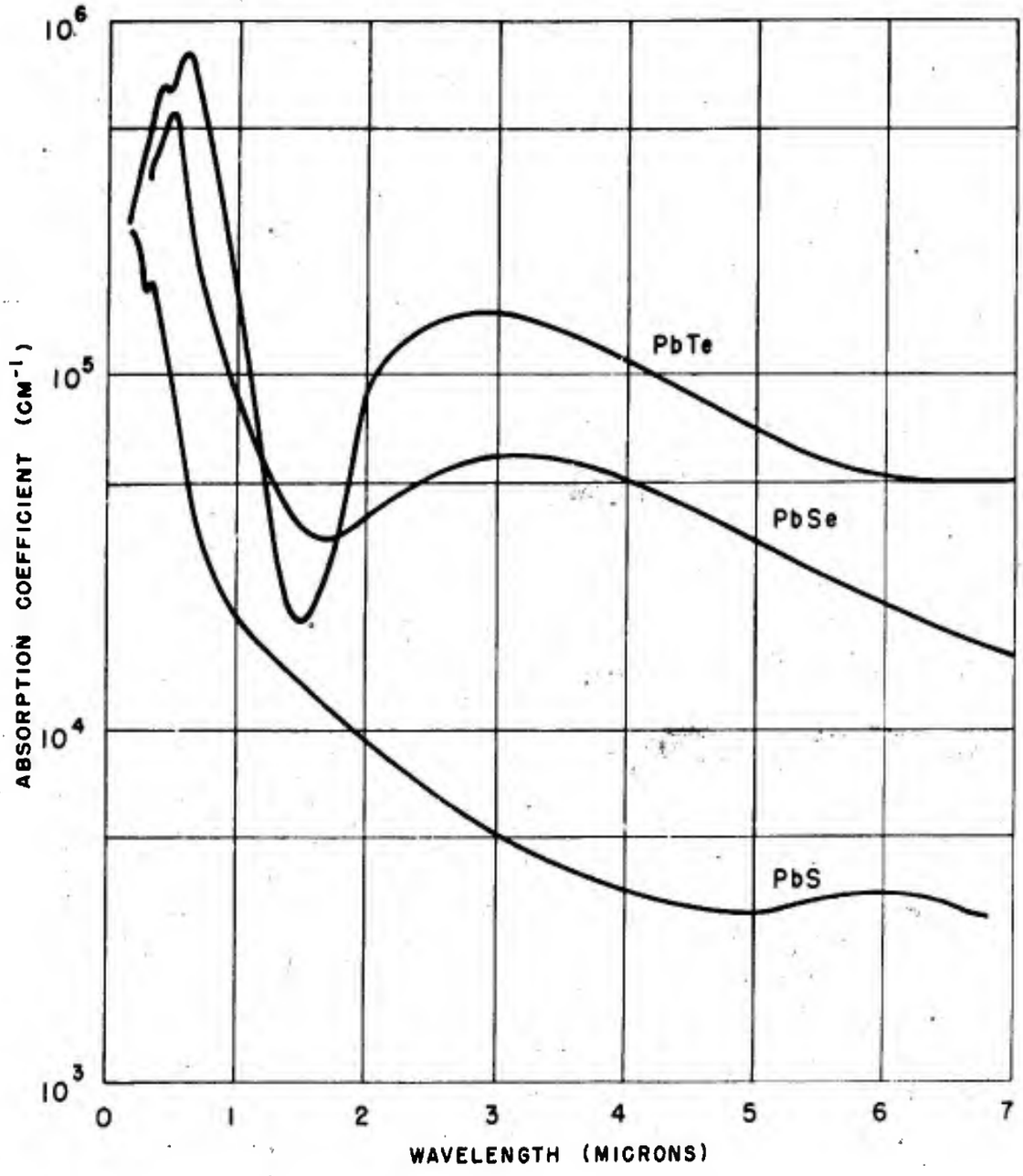

theory". According to the numbers theory the only significant change in conductivity is that produced directly by the increase of the number of free carriers. Thus, $\Delta\sigma = (\Delta n)e\mu$. No important change in mobility is believed to take place. In contrast, the barrier modulation theory states that this increase in number of carriers produces a change in mobility by modifying the height of electrical barriers in the film. Thus $\Delta\sigma = \sum_j [(\Delta n_j)e\mu_j + n_j e(d\mu_j/dn_j)\Delta n_j]$, where $(d\mu_j/dn_j)\Delta n_j$ represents a change in mobility produced by the initial change in carrier concentration Δn_j. If $d\mu_j/dn_j > \mu_j/n_j$ the second term would be the more important one.

In either model sensitivity is normally defined as the fractional change in conductivity $\Delta\sigma/\bar{\sigma}$ for unit incident light intensity. Thus we see that for a given change in carrier concentration Δn the greatest sensitivity will occur when $\bar{n}$ (equilibrium number of carriers in the dark) is small. According to the barrier modulation model this may be modified if $d\mu_j/dn_j$ is not constant.

These two mechanisms are at present in competition for acceptance. Numerous investigations have been made, some tending to support one theory, others supporting the other. No single direct measurement of the relative change of n and μ has yet been reported.

The third process, recombination, has been extensively used as an analytical aid in evaluating particular theories. A carrier can cease to be free to conduct in one of two ways: by direct

recombination with a free carrier of the other type (Shockley & Read)[20] or by trapping (Fan)[21]. Direct recombination takes both carriers out of consideration, reducing the conductivity to its dark value. In this case the lifetimes of the two carriers (majority and minority carriers) are the same. Furthermore, this recombination time is controlled by the concentrations of free holes and electrons. Any temperature dependence will be due to concentration changes.

On the other hand, trapping of one carrier leaves the other free to conduct for the duration of the trapping. Thus in p-type material when an electron (minority carrier) is trapped it cannot act to reduce the number of conducting holes (majority carriers) to its dark value. The capture time will be controlled by relative concentrations of the carriers and traps, while the escape time will depend on the depth and shape of the trap, and on the temperature through changes in thermal energy of the trapped carrier. We thus see that rapid recombination limits the photoconductive current. On the other hand rapid trapping of the minority carrier will make it possible for the majority carrier to have a long lifetime, if the escape time from the trap is long. This effect will enhance the photoconductivity, since either type of carrier can contribute to the photocurrent.

These three basic processes will now be considered in the light of the results described in CHAPTER IV. We will show what modifications must be made in existing theories in terms of these

processes and in terms of the physical and chemical conditions of the photoconductors. The simplest model consistent with the facts will be sought.

SECTION B. Summary of Present Results

The important results produced by the present study may be summarized as follows:

1. All sensitizing agents examined produced a change of carrier sign from n-type to p-type and a resistivity maximum of approximately the same height, at or near the thermoelectric null point.

2. The resistivity at its peak value is approximately 3 ohm-cm, as compared to 0.1 ohm-cm expected from bulk measurements.

3. At high temperatures the resistance increases with added sensitizer treatment apparently without reaching a maximum.

4. All sensitizers produced sensitivity at room temperature when films had been pretreated with oxygen; no sensitizer except oxygen produced photoconductivity at room temperature when used by itself.

5. All sensitizers tested produced photoconductivity at -195°C.

6. Oxygen-sensitized films showed three time constants at -195°C. Other sensitizers produced only the fastest and slowest of these responses, the intermediate effect being completely absent. At room temperature only one time constant was observed.

Time constants normally decreased with rising temperatures; occasionally in a cell which showed only a fast response at -195°C a second (slower) time constant developed at around -78°C.

7. No significant differences in spectral limit were observed among the various sensitizers.

SECTION C. Formulation of a Model

These facts will now be examined to determine what conclusions can be drawn from them.

We see from item 1 that each sensitizer lowers the Fermi level. It can do this by introducing acceptor levels, either on the surface or within the crystallites. These levels drain off the conduction electrons. Item 2 shows that some sort of surface barriers exist at the high-resistance condition. Item 3 indicates that the barriers are increased in magnitude by the treatment with a sensitizer.

These conclusions are indicated in Fig. 31. In 31a and 31b we show the band diagrams for pure n-type PbSe at -195°C and 25°C, respectively. Two crystallites and the gap between are represented in each diagram of Fig. 31. Barriers exist between the crystallites because of the image forces encountered on moving a carrier out of one crystallite and into the next. These barriers are symmetrical about a horizontal axis.

Figs. 31c and 31d show the effect of a surface layer of oxygen at -195°C and 25°C, respectively. The Fermi level has been

FIG. 31
EFFECT OF SENSITIZERS ON PbSe ENERGY BANDS
INSIDE AND BETWEEN CRYSTALLITES

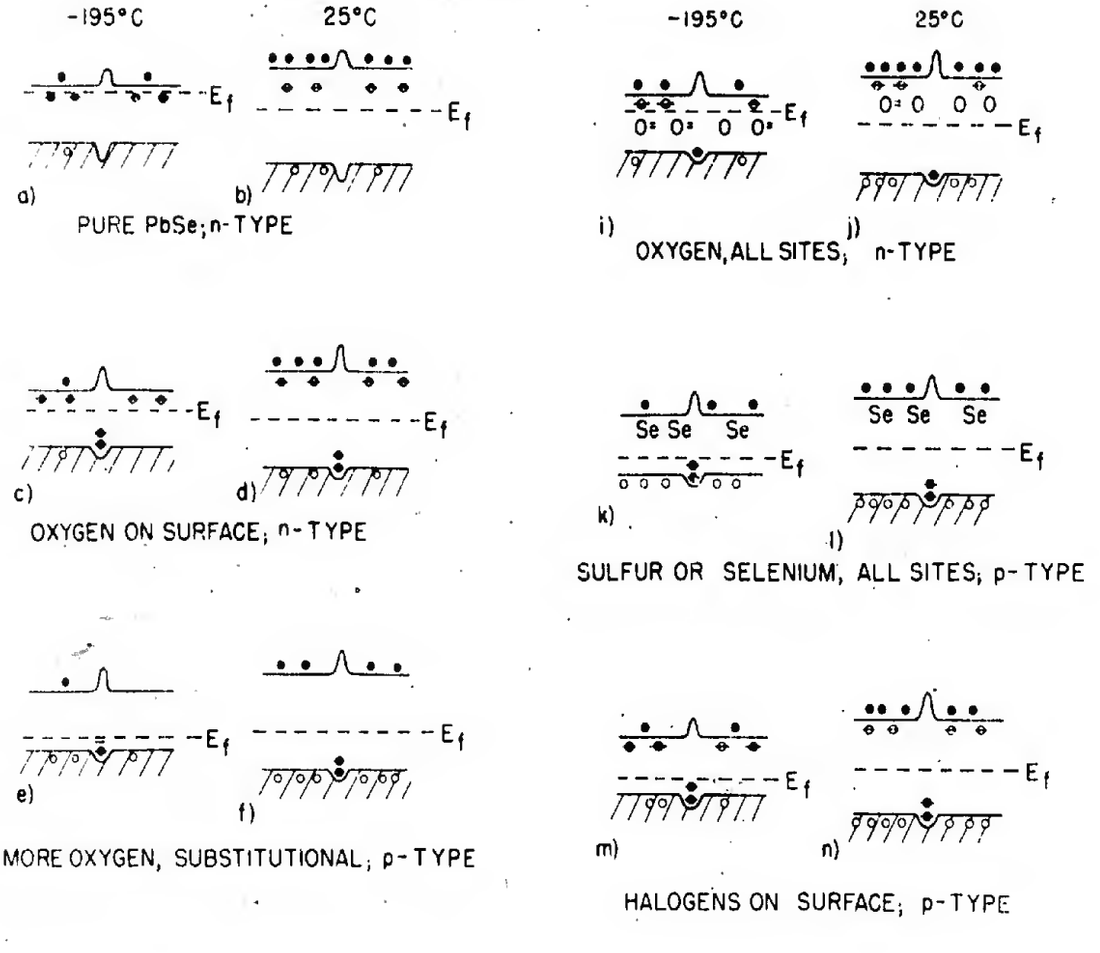

lowered in each case, decreasing the number of free electrons, although the film has not yet been converted to p-type. This will be a fairly high resistance sample. The barriers are now higher for electrons than for holes, because of the surface charges. This assymmetry may give rise to the differences observed between the resistance-temperature curves for n-type and p-type material.

Returning to the summary in SECTION B, item 4 taken with item 1 is a most important factor, since it indicates that a simple decrease of dark conductivity is not sufficient to produce photoconductivity, even in the presence of surface barriers. We must thus look further for an explanation of the difference.

Smith[22], Gibson[23], and their co-workers have advocated the barrier modulation theory, to meet previous inadequacies of numbers theories. Since the specific models presented were based on the value of 1.2 ev for PbS, they cannot now be applied in their original form. Modifications have not yet been presented, but Smith states in a recent survey paper[24] that he believes the photoconductivity is closely tied up with the trapping of carriers in surface states.

The surface barrier explanation does not seem adequate to explain the present facts, however. Fluorine treatment was found to convert n-type thin films to p-type, just as oxygen does; but it was also found to have no effect on the resistance of a thick film, while oxygen was equally effective against thick and thin

films. This suggests that in a very thick film surface barriers are incapable by themselves of depressing the Fermi level, but that oxygen is able to diffuse into the crystallites, converting the whole interior to p-type. Furthermore, it seems quite unlikely that the surface barriers produced by fluorine or chlorine could be significantly different in trapping action from those produced by oxygen, since all three elements are highly electronegative, the value for oxygen (3.5 ev) lying between those of fluorine (4.0 ev) and chlorine (3.0 ev).

We are thus led to consider whether significant trapping within the crystallites could be expected to occur in the case of oxygen treatment but not in other cases. Bode and Levinstein[25] suggest that such interior traps exist in PbTe, but are normally filled and ineffective. The action of oxygen would be to lower the Fermi level by producing surface acceptor states, thus draining the traps. Then when electron-hole pairs are excited optically the electron (minority carrier) will be trapped, preventing recombination. The photoconductive current is by holes; the time constant observed would correspond to the time required for the electron to escape from the trap and recombine. No barrier modulation is required even though the surface levels play an important role in sensitization.

This model also fails to explain adequately the present results, since all the sensitizers lower the Fermi level. Thus if the traps existed prior to sensitization, any treatment which

adequately lowers the Fermi level will empty them and improve the lifetime in the same way as oxygen does.

Consideration of the above points has led to the conclusion that oxygen must be capable of introducing traps into the interior of the crystallites, in addition to producing surface states which lower the Fermi level. If oxygen diffuses into the crystallites some of it will go into the selenium vacancies. This condition is shown in Figs. 31e and 31f (-195°C and 25°C). The Fermi level has been lowered sufficiently to make the film p-type. The barriers are still symmetrical, but still limit both electron and hole mobilities. The oxygen ions will fit easily into the selenium vacancies, distorting the potential slightly by virtue of the small ion radius; but still it will be a neutral impurity with no strong tendency to attract more electrons.

Those oxygen atoms which enter interstitial positions, on the other hand, may act as electron traps. There is enough space available to accommodate an oxygen atom interstitially, without seriously distorting the lattice, but not an $O^{=}$ ion, because the ion radius is about twice that of the atom. On the other hand the atom gains energy by capturing electrons, as shown by its high electronegativity. Thus the equilibrium ratio of interstitial ions to interstitial atoms depends on the temperature, the difference ϵ between the gain of energy by ionization and the work done against the lattice by the expanding ion, and on the number of available electrons (i.e., the position of the Fermi level). Any

oxygen remaining as an atom can act as an electron trap and capture electrons excited optically. The length of time the electron will remain trapped (escape time constant) will depend on ϵ and temperature.

The energy diagrams for the situation just described are shown in Figs. 31g and 31h. Because the material is p-type a large percentage of the interstitial oxygen is found as atoms even at low temperatures.

One further process which has not been discussed specifically is the process of recombination. This process takes place in all samples whether sensitized or not; indeed it is the process which prevents photoconductivity in a high-resistance sample without interstitial oxygen. Thus we must assume that it is a property of the lattice. We will assume that it is due to lattice defects in the crystallites, or some similar imperfection. The action of physical recombination centers is to provide a mechanism by which the free electrons may lose their energy and momentum to the lattice and return to the valence band.

SECTION D. Summary of the Model

Now let us summarize the model arrived at by the above process. First of all, we maintain the following features from previous work:

1. Absorption of light producing photoconductivity takes place in the body of the crystallites.

2. The effect of absorption is normally to create a hole-electron pair, raising the electron across the forbidden gap.

3. Excess lead atoms or selenium vacancies are donor impurities; lead-vacancies are acceptor impurities. These levels are close to the conduction and valence bands, respectively. If both types are present only that type occurring in the higher concentration produces free carriers (compensation).

In addition we assume the following:

4. Imperfections such as lattice defects act as recombination centers, producing rapid recombination of optically created electron-hole pairs. The minimum concentration of these defects can be calculated from thermodynamic arguments.

5. Oxygen may become attached to the surface of the film, or enter selenium vacancies or interstitial positions. Of these three, only interstitial oxygen acts to produce room temperature photoconductivity. Its action is to trap the optically-freed electrons, leaving the excess holes free to conduct. Escape of the electron from the oxygen permits direct recombination, which stops the photocurrent.

CHAPTER VI

ANALYSIS OF THE MODEL

SECTION A. Photoresponse, Time Constant, and Temperature Dependence

Now let us consider the effect of illumination on such a system. Recall first the expression for the rise of photoconductivity given in Eq. 3 (CHAPTER IV B) for monomolecular recombination:

$$\Delta n = \frac{\alpha I \tau}{[1+(\omega\tau)^2]^{1/2}} \qquad (3)$$

The sensitivity $\Delta n/\bar{n}$ is proportional to the time constant τ at low frequencies, and inversely proportional to the carrier concentration in the dark. We must examine each case to determine what value of τ will be found.

Consider first the effect of illumination on the pure samples of Fig. 31a at -195°C. A photon absorbed by the PbSe will create a hole-electron pair, thus lowering the resistance. Because of the presence of the recombination centers the electron will easily lose its excess energy to the lattice and then recombine with a hole. The time constant associated with this is identified with the observed 20 microsecond time constant (τ_1). The same behavior would exist whether the film were slightly n-type,

stoichiometric, or p-type. Because of the lower value of $\bar{n}$ the sensitivity will be highest for stoichiometric samples.

Now consider the same material at 25 °C. $\bar{n}$ is larger than it is at -195°C; in addition, the recombination time constant τ_1 is smaller, partly because thermal motion has increased the recombination cross section, but principally because the number of recombination centers has increased. The combined effect of these two factors $\bar{n}$ and τ_1 is to reduce the attainable sensitivity to a level too low to be measured.

When oxygen has entered the lattice interstitially as in Fig. 31g to 31j (p-type samples) another process takes place. As stated above, the oxygen atom may trap electrons, becoming $O^=$. Those which have not become ions may act as traps for electrons excited optically. When a hole-electron pair is created, the electron will be attracted by some oxygen atom becoming trapped, and leaving the hole free to conduct. The time constant τ_2 for release of the electron from the ion is long compared to the recombination center value τ_1. τ_2 is identified as the 5 millisecond time constant observed at -195°C in stronglyp-type materials, as reported in CHAPTER IV B. It is to be noted that the time constant for trapping an electron must be comparable with τ_1 or faster, if the trap is to compete successfully with the recombination centers. On the other hand the photoresponse is proportional to the time constant for release of the trapped electron, since the extra hole is free to conduct until the

electron escapes from the trap and recombines. Hence the criterion for behavior of a trap as an effective sensitizer must be a very short capture time and a relatively long release time.

Now consider the effect of warming the sample to 25°C, as shown in Fig. 31h. The dark concentration $\bar{n}$ of course increases and τ_1 decreases as described previously. In addition, as the Fermi level rises a larger fraction of the interstitial oxygen atoms become $O^=$ ions. This reduces the total statistical probability of capture of optically excited electrons by oxygen atoms. In addition the time constant of release of trapped electrons decreases. This lowers the value τ_2 entering the sensitivity equation. Thus we have four effects acting to decrease the photosensitivity.

This explains why it is possible to obtain a conversion from n- to p-type conductivity and achieve a resistance maximum without obtaining photosensitivity. If there are no interstitial oxygen atoms the recombination takes most or all the photoelectrons back to the valence band too quickly to produce photoconductivity. Precisely this action is believed to explain the behavior observed upon treatment with sulfur, selenium, and the halogens, as will be seen below.

There is a further effect which occurs in a p-type system such as that shown in Figs. 31e or 31g. The surface states have drained off conduction electrons and increased the height of the barriers to electron flow, thus lowering the dark mobility. The

Fermi level is low enough that some of the surface states are unfilled. These will act as electron traps, attracting electrons freed by radiation, thus leaving the corresponding hole free to conduct. These levels have very long time constants (τ_3) because of the presence of the barriers, and are responsible for the effects classed as "frozen-in photoconductivity".

If the film is now warmed, the levels are further filled, but the importance of the barriers as compared to the thermal energy of the trapped electrons decreases. Thus, the time constant of recombination from the levels decreases. If the material is again recooled the levels empty at a rate determined by the instantaneous temperature, the rate of lowering of the Fermi level, and the barrier height. Thus the levels are again capable of trapping optically freed electrons.

There is one further condition of interest produced by oxygen treatment: photoconductivity in n-type films. The condition is shown in Figs. 31i and 31j. We note that at low temperatures the Fermi level is high, thus causing a large fraction of the interstitial oxygen to become $O^{=}$. Hence the number of atoms remaining to be effective as electron traps is small. Accordingly τ_2 will not be seen to any significant amount, most of the optically freed electrons combining through the recombination centers. As the material is warmed, however, the number of ions will decrease and the number of optical electrons trapped will increase. Thus τ_2 will become important. This may result in the occurrence

of two time constants at intermediate temperatures, one of which is longer than that observed either at higher or lower temperatures in the same sample.

If the film is then warmed further to 25°C as shown in diagram (j), a further decrease of τ_1 and τ_2 will take place. The contribution to the photoconductivity before time τ_1 becomes vanishingly small. At this temperature τ_2 is shorter than the -195°C value of either τ_1 or τ_2.

SECTION B. Effect of Other Sensitizers

Now consider the effect of treatment with sulfur or selenium. It is assumed that either element can enter the film filling selenium vacancies or occupying interstitial sites. Also surface layers may be produced. The results of surface levels and substitional ions are exactly comparable to those described for oxygen. Both τ_1 and τ_3 are observable. However, the $S^=$ and $Se^=$ ions are much larger than the $O^=$ ions, and the electronegativity of sulfur and selenium is much less than that of oxygen. Thus the net energy gain of an interstitial sulfur or selenium atom on capturing an electron is much less than that of an oxygen atom. Thus trapping of electrons by interstitial atoms is much less likely to take place, and no τ_2 component of photoconductivity will arise either at -195°C or 25°C. This is just what is observed.

In the case of treatment with the halogens it is believed that no diffusion into the film takes place. The evidence for this is the high electronegativity of F_2 and Cl_2. If either atom entered substitutionally or interstitially the large electronegativity should guarantee trapping of electrons, giving rise to the presence of a τ_2 component both at -195°C and 25°C, neither of which is observed. However, the τ_1 and τ_3 effects are both present at -195°C.

Furthermore, attempts to change the position of the Fermi level by fluorine treatment of thick (opaque) films was unsuccessful. This indicates that no diffusion into the film took place, and that in the thick film a surface layer is incapable of affecting significantly the position of the Fermi level. The explanation of the τ_3 effect is unchanged from that given in the case of oxygen treatment.

In the case of pretreatment with oxygen followed by halogen treatment, the oxygen electron traps are introduced into the material and not removed by baking in vacuum. Sufficient selenium atoms must evaporate from the lattice during the vacuum baking to produce n-type material. Then the production of surface states by the halogen lowers the Fermi level and produces a high resistance, and the oxygen levels produce the proper time constant τ_2. Figs. 3li and 3lj apply directly.

CHAPTER VII

THEORY OF THE EFFECT OF FILM THICKNESS ON RESPONSIVITY AND SIGNAL-TO-NOISE RATIO

SECTION A. The Relation Between Absorption and Photoconductive Response

It was indicated in an earlier section that a noticeable extension of the photoconductive limit to longer wavelengths had been achieved by using thicker films. Although this was reportedly due to the presence of absorption in this spectral region no absorption data adequately explaining the behavior was then available. The absorption data could not be reconciled satisfactorily with the evidence of photoconductive spectral sensitivity. One purpose of this investigation was to determine whether some procedure was normally used in sensitizing thin films which inhibited their long wavelength photoconductivity, or conversely whether some procedure was possible in sensitizing thick films which gave rise to a new photoconductive limit impossible in thin films, such as the introduction of new energy levels.

No evidence for either such phenomenon was found in this experimental study. Furthermore, we will show in this section that the extension of the photoconductive limit to longer wavelengths can be explained as an intrinsic property of lead

selenide, directly related to film thickness. No new absorption levels are necessary to explain the observed results. In order to show this we first derive an expression which relates the photoconductive response to the absorption coefficient and the film thickness.

There are two ways in which sensitivity can be defined. One way considers only the magnitude of signal obtainable. Thus the "responsivity" of such a detector is defined as the output signal voltage per unit intensity of incident radiation. The second way considers both signal and noise voltage, and relates to the minimum signal power detectable by the device. The signal-to-noise ratio is quoted in terms of unit incident power; the minimum detectable power is defined as that incident power capable of producing a signal equal to the noise of the detector. The importance of signal-to-noise ratio operationally is that it represents a limit which cannot be overcome by the use of more gain, quieter amplifiers, etc.

The basic circuit in which a photoconductive detector is used is shown in Fig. 32. A dc voltage V_o is applied across the cell R_c and a load resistor R_L normally equal to the equilibrium cell resistance $\bar{R}_c$. It is shown in the appendix, Eq. (A14), that if a beam of I_o photons per cm.^{2} per second falling on the sample is chopped at a frequency $\omega/2\pi$, an ac signal voltage V_{ac} is developed, given by

$$V_{ac} = \frac{V_o}{4}\frac{\Delta G}{\bar{G}} = \frac{V_o}{4}\frac{I_o}{\bar{n}}\frac{\tau}{[1+(\omega\tau)^2]^{1/2}}\left(\frac{1-e^{-ad}}{d}\right) \qquad (5)$$

Here $\bar{G}$ = conductance of the sample in the dark

ΔG = change of conductance on illumination

$\bar{n}$ = equilibrium concentration of carriers in the dark

α = absorption coefficient

d = film thickness.

V_{ac} is seen to be proportional to $\Delta G/\bar{G}$, which we previously defined as photoconductive sensitivity (CHAPTER I B).

Consider the effect on $\Delta G/\bar{G}$ of varying the film thickness d. Expanding the exponential term in Eq. (5) we obtain

$$\frac{\Delta G}{\bar{G}} = \frac{\tau I_0}{\bar{n}[1+(\omega\tau)^2]^{1/2}} \left\{ \frac{\alpha d - \alpha^2 d^2/2! + \cdots}{d} \right\} \qquad (6)$$

$$\therefore \lim_{d \to 0} \frac{\Delta G}{\bar{G}} = \frac{\tau I_0 \alpha}{\bar{n}[1+(\omega\tau)^2]^{1/2}} \qquad (7)$$

Hence

$$\lim_{d \to 0} \frac{\Delta G}{\bar{G}} = K\alpha \qquad (8)$$

where K is a proportionality factor independent of λ and d.

Thus the responsivity of a very thin film should be directly proportional to the absorption coefficient α. Any wavelength dependence of $\Delta G/\bar{G}$ in such a film should be explainable in terms of a wavelength dependence of α.

SECTION B. Comparison of Observed Absorption Data with Photoconductive Response

The work of Scanlon[18], Gibson[17], and Avery[19] has clarified the question of the basic absorption process involved in photo-

conductivity; i.e., that the energy gap obtained from the photoconductive limit in PbS corresponds to main-band absorption rather than to impurity absorption. This limit is not in agreement with the film absorpiton measurements of Gibson[15], which show no edge except that near 1 micron. Because transmission measurements in thin films are complicated by scattering and surface effects we discard this film absorption data in favor of the better evidence of crystals.

Avery's data taken from crystal reflection measurements (converted to absorption coefficient[26]), together with Gibson's crystal absorption measurements[17] are reproduced in Fig. 33. In Fig. 34 we have applied Eq. (5) to Avery's data for various values of film thickness d. We see that in the thin films there is no knee at 3.3 microns comparable to that normally seen in the photoconductive data. Furthermore, there is only a very slight shift of position of the knee with thickness, due to the steepness of the edge. Thus these data do not predict the photoconductive data.

SECTION C. Main Band Absorption Expressions

Expressions for absorption based on the transition probability for creating an electron-hole pair across an energy gap ΔE have been developed recently by Dexter[27], and by Bardeen, Blatt, and Hall[28]. In these developments, it is seen that radiation of energy E greater than the band gap energy by an amount ϵ will be absorbed and create an electron-hole pair with

a probability

$$K \propto \epsilon^n \tag{9}$$

where n is some positive exponent whose value depends on the shape of the energy-momentum surfaces and the type of transition involved. Thus for spherical energy contours the values n = 1/2 or n = 3/2 are obtained. If, on the other hand, the energy-momentum surfaces have multiple maxima and minima, the exponent depends on whether or not selection rules based on conservation of momentum are obeyed. Transitions in which the selection rules are obeyed are termed direct, those in which they are violated are termed indirect. Direct transitions require the values n = 1/2 and n = 3/2, while values of n from 1 to 3 are predicted for the indirect cases, depending on the conditions.

Since the absorption coefficient is proportional to the transition probability this gives us

$$\alpha = C\epsilon^n = C\left(\frac{hc}{\lambda} - \Delta E\right)^n. \tag{10}$$

Fan, Shepherd, and Spitzer[29] report experimental absorption measurements in germanium showing an $\epsilon^{2.5}$ dependence. In Fig. 35 Eq. (10) is plotted in terms of wavelength, for values of n of 1/2, 1, 2, and 3, and for λ_c = 3.3μ and 5μ corresponding to ΔE = 0.37 ev and 0.25 ev respectively.

FIG. 32
CIRCUIT FOR RESPONSIVITY
AND S/N CALCULATION

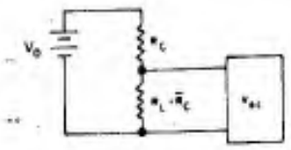

FIG. 33
ABSORPTION COEFFICIENT
IN PbSe CRYSTALS

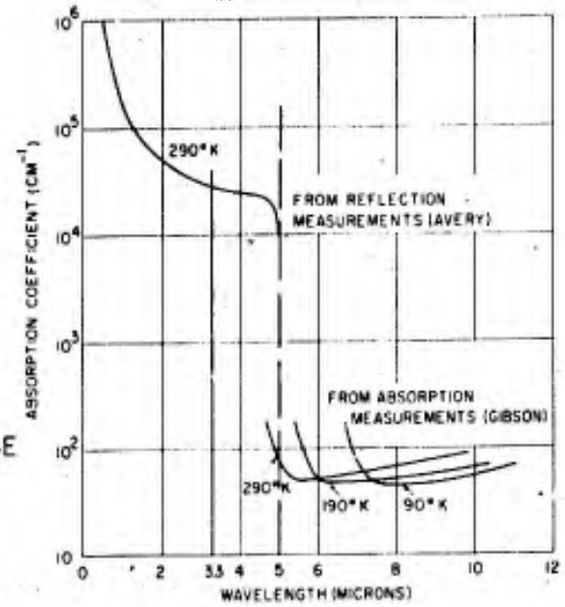

FIG. 35
THEORETICAL WAVELENGTH DEPENDENCE
OF BAND-TO-BAND ABSORPTION
FOR VARIOUS BAND SHAPES

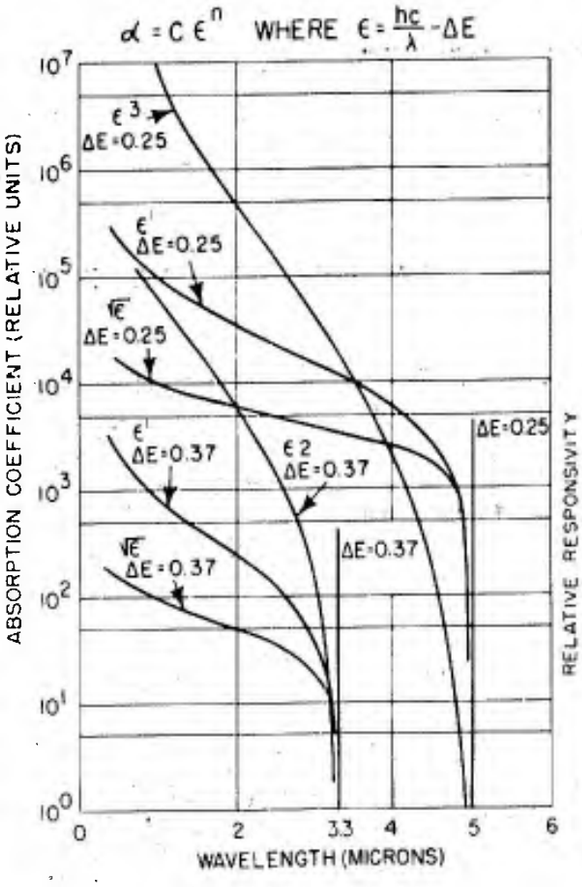

FIG 34
EFFECT OF THICKNESS ON RESPONSIVITY
AVERY CRYSTAL REFLECTION DATA

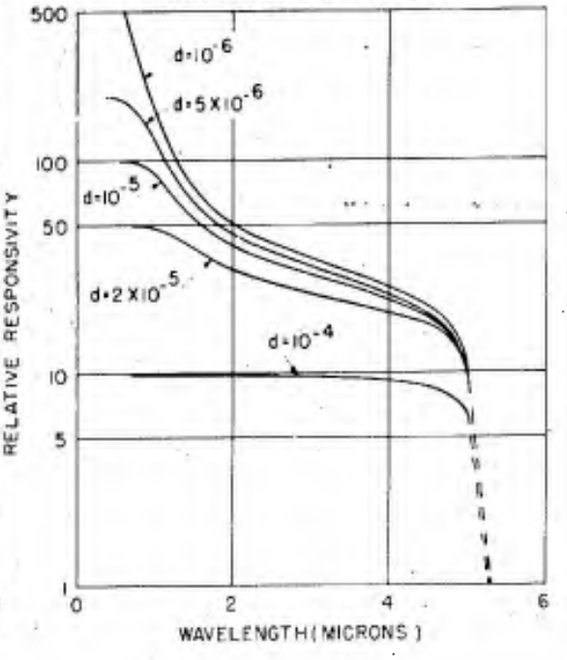

SECTION D. Comparison of Photoconductive Response Data and Theoretical Absorption Expressions

The absorption we are concerned with is main-band absorption; because of this we have theoretical predictions as to the possible functional dependence of α on λ. Furthermore Eq. (8) shows that in the limit of thin films the photoconductive sensitivity $\Delta G/\bar{G}$ is proportional to α. Thus we make the hypothesis that the correct one of the various expressions predicted for main-band absorption is that one which most closely agrees with the shape of the $\Delta G/\bar{G}$ vs. λ curves observed for thin films. To see which expression this is, we plot the observed $\Delta G/\bar{G}$ for several thin films against $\epsilon = (hc/\lambda - \Delta E)$, on a logarithmic plot. Fig. 36 shows the result. We see that the long-wavelength data for a given cell can be represented fairly well by a straight line, indicating a power law $\Delta G/\bar{G} \propto \epsilon^n$, with n ranging from 2 to 4, with three of the cells yielding a value very close to $n = 3$. The cells reported were prepared and measured in three different laboratories, so the range of exponents is not surprising.

In Fig. 37 we have replotted on a common scale an observed photoconductive response curve and the curves for $\epsilon^{1/2}$, ϵ, and ϵ^3. We see that the long wavelength edge of the photoconductive response curve corresponds rather well to the shape of the ϵ^3 curve, indicating that the photoconductive response represents the result of indirect-transition main-band absorption.

Accordingly we assume that the true absorption coefficient can be derived from the photoconductive response curve observed in very thin films. We set the value of the absorption coefficient at short wavelengths (2 microns) to correspond roughly to the values indicated in this wavelength region by Gibson[15]; the value at any other wavelength is then obtained from this by use of the observed wavelength dependence of photoconductivity.

We may then apply Eq. (5) to this curve, for various values of film thickness (assuming $\omega = 0$), to see whether it predicts correctly the observed response of thick films, with the shift of the knee to longer wavelengths. The results of this calculation are shown in Fig. 38.

We see that the behavior predicted for thick films agrees well with experiment; both the shift of the knee, and the loss of short wavelength sensitivity are predicted. Fig. 38 shows that the only effect increased film thickness can produce on the magnitude of $\Delta G/\bar{G}$ is to reduce it. That is, making the film thicker will not increase the value of $\Delta G/\bar{G}$ at any wavelength.

The absorption observed by Gibson in the range from 5 microns to 10 microns was attributed to free carrier absorption. In Fig. 37 we have included an estimated level of free carrier absorption, carrying it back through the band edge at 5 microns. By adding this absorption to the absorption given by the ε^3 law, in the range from 4.5 to 5.0 microns, the dashed portion of the curve is obtained. This curve has the same shape as Gibson's measured crystal absorption in this region.

Smith[24] has described a calculation by G. G. MacFarlane, in which he used a similar extrapolation to determine ΔE. MacFarlane fitted the long wavelength portion of the crystal absorption data of Gibson by a quadratic in λ, and extrapolated back to short wavelengths. Subtracting the extrapolation from the measured values yielded a curve which agreed nicely with Eq. (10) for n = 3. He obtained ΔE = 0.22 ev at 25°C, corresponding to a cut-off wavelength λ_c = 5.6 microns.

Although we are attributing the shape of the long wavelength edge of the absorption curve (photoconductive response curve) to indirect transitions, we can expect that direct transitions will take place at shorter wavelengths. These should obey an $\varepsilon^{1/2}$ or $\varepsilon^{3/2}$ law, where the ΔE used is greater than that for the indirect transitions. This ΔE is the energy gap corresponding to the case where the momentum selection rules are observed. Its value has not been determined experimentally. However, the photoconductive knee has not been observed to move to wavelengths shorter than 3.3 microns, even for films of very small thicknesses. It thus is rather likely that the edge corresponding to direct transitions is in this neighborhood.

If this edge is at 3.3 microns we would expect any fairly thin film to have a peak in the response around 1 micron, a plateau extending from about 1.5 microns to 3 microns, and a definite knee at 3.3 microns (i.e., the shape of the curve $\varepsilon^{1/2}$ for ΔE = 0.37 ev.). The edge from 3.3 microns to 5 microns would be due to a combination of direct and indirect absorption.

This shape would be the same for all films thin enough that complete absorption of the 3 micron radiation does not take place. A thicker film would show the results indicated in Fig. 38. An actual calculation of the combined absorption resulting from direct and indirect transitions would depend on being able to choose the relative amplitudes of the two components. The photoconductive data are not good enough at the present time to attempt such a calculation.

SECTION E. Signal-to-Noise Ratio

Since photoconductive sensitivity is frequently expressed in terms of a signal-to-noise ratio, it is of interest to determine how this will depend on film thickness. To do this, we will make use of a calculation of Petritz[30] which expresses the electronic noise in terms of fundamental quantities. He shows that the noise current is,

$$\sqrt{G(\Delta i^2)} = \frac{eE\mu}{L}\left[\frac{2\tau\bar{n}Ad\,\Delta f}{1+(\omega\tau)^2}\right]^{1/2} \qquad (11)$$

where $\sqrt{G(\Delta i^2)}$ is the noise current, E is the applied field strength, A is the sensitive area, L is the film length in the direction of current flow, Δf is the frequency pass band, and the other symbols are as we have used them above.

Eq. (A12) in the appendix gives signal current in terms of conductance change ΔG. Inserting the explicit form of ΔG from Eq. (A9) into (A12) and using $V_o/2 = EL$, we obtain

$$i_{sig} = \frac{EL}{2}\,\frac{W}{L}\,\frac{e\mu\tau I_o(1-e^{-\alpha d})}{[1+(\omega\tau)^2]^{1/2}} \qquad (12)$$

$$= \frac{EA}{2L}\,\frac{e\mu\tau I_o(1-e^{-\alpha d})}{[1+(\omega\tau)^2]^{1/2}}. \qquad (13)$$

This represents the current change produced by illumination chopped at frequency $\omega/2\pi$.

Thus signal-to-noise ratio is obtained by combining Eqs. (13) and (11):

$$\frac{S}{N} = \frac{i_{sig}}{\sqrt{G(\Delta i^2)}} = \frac{I_o A(1-e^{-\alpha d})}{2[2\bar{n}Ad\Delta f/\tau]^{1/2}} \qquad (14)$$

$$= \left[\frac{\tau A}{8\bar{n}d\Delta f}\right]^{1/2} I_o(1-e^{-\alpha d}) \qquad (15)$$

Note that whereas thickness d appeared as $(1-e^{-\alpha d})/d$ in $\Delta G/\bar{G}$, Eq. (5), it appears as $(1-e^{-\alpha d})/d^{1/2}$ in S/N.

Eq. (14) is plotted in Fig. 39 with thickness as abscissa and wavelength (and absorption coefficient) as a parameter using the wavelength-absorption coefficient relation shown in Fig. 38. We see that for low absorption coefficients (long wavelengths) there is a good deal to be gained by going to thicker films, if S/N rather than responsivity is important.

FIG. 36
RESPONSIVITY AS A BAND-TO-BAND TRANSITION

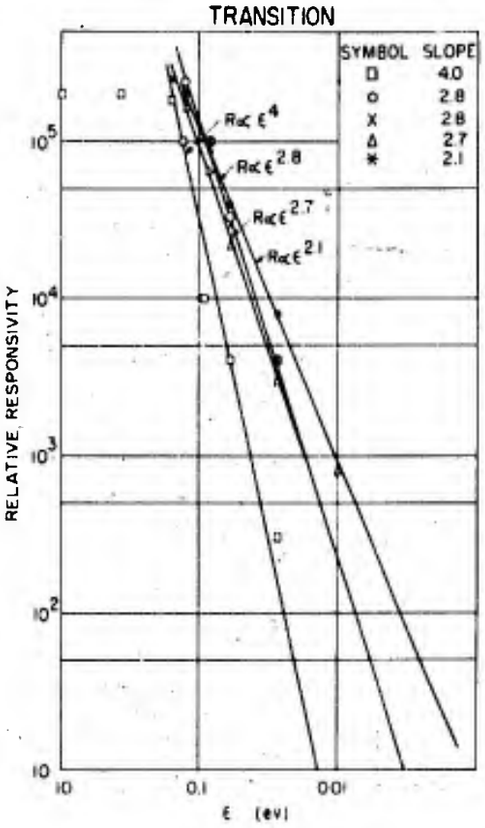

FIG. 37
COMPOSITE ABSORPTION CURVES

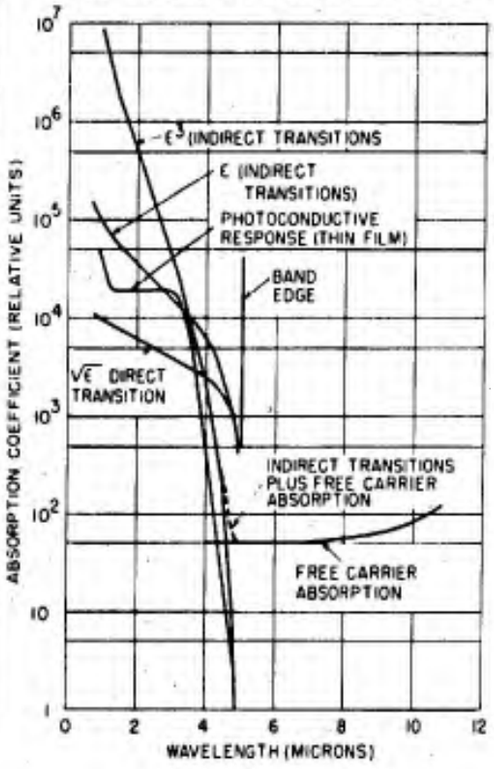

FIG. 38
EFFECT OF THICKNESS ON RESPONSIVITY
(ABSORPTION COEFFICIENT DERIVED FROM PHOTOCONDUCTIVITY)

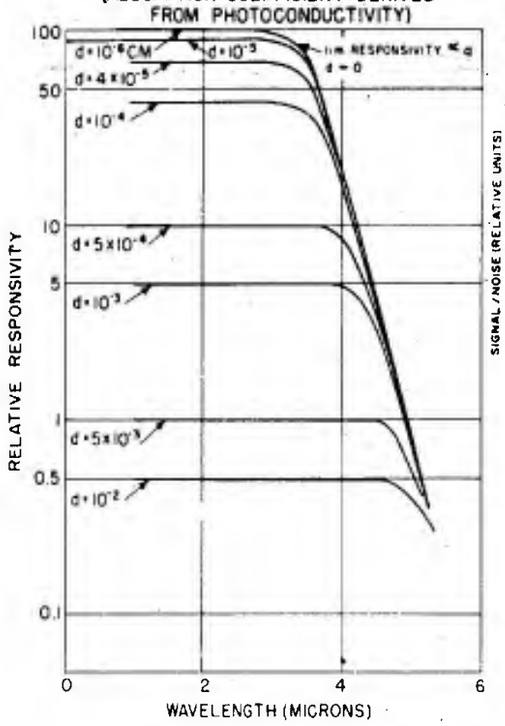

FIG. 39
EFFECT OF THICKNESS ON SIGNAL/NOISE
(CALCULATED FROM PHOTOCONDUCTIVE DATA)

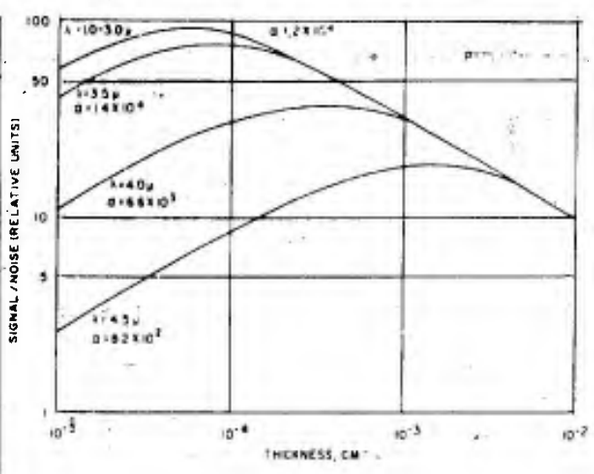

CHAPTER VIII

SUMMARY AND CONCLUSIONS

A study of various parameters accessible to control in the preparation of photoconductive layers of PbSe has been made. Parameters varied are starting materials, film thickness, heat treatment, sensitizing agents, and operating temperatures. Seven different sensitizing agents were used. Previously, investigation of only one of these sensitizers had been reported.

Various existing models were considered and found to be inadequate to explain the new information. A new model was developed which is qualitatively in harmony with both previous and present experiments.

The model suggested for the photoconductive process is the following. The absorption of light by the crystallites creates free hole-electron pairs. One or more of the following processes will then take place: (a) lattice defects provide a mechanism for fast recombination of electrons with holes; until this happens both holes and electrons carry the photoconductive current; (b) interstitial oxygen atoms trap the electrons for a short time, permitting the holes to carry a photoconductive current until the electrons escape and recombine; (c) surface levels trap electrons for an extended time during which the holes are free to carry the photoconductive current.

Of all the sensitizers studied, only oxygen produced mechanism (b), while (a) and (c) were observed for all sensitizers.

Two especially significant points are brought out by these experiments and the model developed from them. First, we see for the first time that the sensitizing mechanism in PbSe is within the bulk material and not in a surface barrier. Second, we now understand the effect of film thickness on sensitivity and spectral response. These points are important enough that a final review of the situation is indicated.

By 1950, various investigators were supporting the view (based on studies of PbS) that both the absorption of the radiation and a change of mobility take place in surface layers on the crystallites. In 1953 Scanlon definitely showed that the absorption is a main-band absorption and therefore takes place within the body of the crystals. The work of Bode (1954) showed that bulk lifetimes are important, but was interpreted to show that the sensitization process consisted of the adsorption of oxygen onto the surface, thus increasing the dark resistance by a simple lowering of the Fermi level. Since Bode's work was all performed at -195°C this is in agreement with the present findings at that temperature. Finally, we have shown that in order to be effective at room temperature the sensitizing agent must enter the bulk material and change the lifetime of the majority carrier by trapping the minority carrier internally; a change of surface barriers is important as a means of lowering the dark conductivity, but by itself is not enough to produce observable

sensitivity.

The present experiment does not give any evidence as to whether or not barrier modulation may take place in addition to bulk trapping. As previously indicated a direct measurement of the Hall effect under illumination should enable us to answer this question. Because of the complexity of the system, no quantitative experimental checks of the theory have been made.

A mathematical investigation of the effect of film thickness on absorption and on photosensitivity was made; published experimental data on absorption and photosensitivity, original experimental data on photosensitivity, and published theoretical expressions for direct and indirect transitions capable of producing absorption were considered. Good agreement was shown to exist between theory, photoconductive data, and absorption data for crystals at long wavelengths. Published absorption coefficients calculated from reflectivity data for crystals in the near infrared and film absorption data throughout the infrared were seen to disagree with theory and photoconductive experiments. A method of estimating the wavelength dependence of the band-to-band absorption coefficient experimentally is suggested.

It is believed that it may be possible to introduce some sensitizers other than oxygen into the lattice in such a way as to produce mechanism (b), but no method of accomplishing this has been found. A study of other elements and other introduction techniques would seem to be indicated.

To check the model quantitatively certain other experiments may be valuable. A measurement of the Hall effect as a function of temperature and illumination will identify the concentration, position, and type of the impurity levels, as well as give evidence as to the existence of barrier-modulation. Such measurements should be made at the various stages of processing of a film using various of the sensitizers studied here.

Quantitative measurements of the amounts of sensitizer taken up by the film should be correlated with the Hall measurements to check the relative importance of the sensitizer compared to previously existing imperfections or impurities.

The model may be analyzed to obtain expressions for the time constant, noise, and responsivity as functions of applied field, light intensity, temperature, and impurity concentration. Such an analysis should follow the study of the Hall coefficient. Experimental measurements suggested by the expressions could then be used to extend or modify the model.

APPENDIX

DERIVATION OF THE EXPRESSION FOR PHOTOCONDUCTIVE RESPONSE

The differential equation relating the change in number of free carriers, $n(x)Adx$, in a layer dx to radiatio.. incident on the layer is, for small changes (monomolecular recombination):

$$\frac{d[n(x)Adx]}{dt} = \alpha I(x) A dx - A[n(x) - \bar{n}]dx/\tau \qquad (A1)$$

where A = area illuminated

α = absorption coefficient

I(x) = number of photons per unit area reaching depth x per second

n(x) = density of free carriers at x

$\bar{n}$ = equilibrium density of free carriers in the dark

τ = time constant for recombination.

The first term on the right represents the rate of releasing carriers by the radiation, and the second term represents the rate of recombination. The solution for this differential equation at equilibrium is

$$n(x) = \bar{n} + \alpha I(x) \tau. \qquad (A2)$$

If the illumination is chopped at a frequency $f = \omega/2\pi$ the maximum value of n(x,t) achieved is

$$n(x,t)_{max} = \bar{n} + \alpha I(x) \tau / [1 + (\omega\tau)^2]^{1/2} \qquad (A3)$$

The conductance G of a film of length L, width W, is

$$G = \frac{W}{L}\int_0^d \sigma(x)\,dx. \tag{A4}$$

Inserting $n(x)-\bar{n} = \Delta n(x)$ and assuming no barrier modulation this is

$$G = \frac{W}{L}\int_0^d n(x)e\mu\,dx = \frac{W}{L}e\mu\int_0^d [\bar{n}+\Delta n(x)]\,dx. \tag{A5}$$

This can be written as the sum of two terms

$$G = \bar{G} + \Delta G$$

where

$$\bar{G} = \frac{W}{L}\,ne\mu d \tag{A6}$$

is the dark conductivity, and

$$\Delta G = \frac{W}{L}e\mu\int_0^d \Delta n(x)dx$$

$$= \frac{W}{L}e\mu\tau\int_0^d \frac{a\,I(x)\,dx}{[1+(\omega\tau)^2]^{1/2}}. \tag{A7}$$

is the change of conductivity on illumination.

Now according to Lambert's Law, equal thicknesses of a uniform sample absorb equal fractions of the incident radiation: $dI/I = -a\,dx$. Integrating this yields

$$I(x) = I_0 e^{-\alpha x} \tag{A8}$$

Inserting this in Eq. (A7) above gives

$$\Delta G = \frac{W}{L} \frac{e\mu\tau I_0}{[1+(\omega\tau)^2]^{1/2}} \int_0^d \alpha e^{-\alpha x}$$

$$= \frac{W}{L} \frac{e\mu\tau I_0}{[1+(\omega\tau)^2]^{1/2}} \left(1 - e^{-\alpha d}\right). \tag{A9}$$

Thus

$$\frac{\Delta G}{\bar{G}} = \frac{\tau I_0 \left(1 - e^{-\alpha d}\right)}{\bar{n} \left[1+(\omega\tau)^2\right]^{1/2} d}. \tag{A10}$$

If we consider a reflection coefficient R at the two interfaces the expression for ΔG is

$$\Delta G = \frac{W}{L} \frac{e\mu\tau I_0}{[1+(\omega\tau)^2]^{1/2}} \frac{(1-R)\left(1-e^{-\alpha d}\right)}{\left(1-Re^{-\alpha d}\right)}. \tag{A11}$$

This correction has been found to be unimportant to the conclusions to be reached below and will not be discussed further.

We now consider the electrical circuit in which such a photoconductor is used. The responsivity of the detector is defined as the output signal in volts resulting when a radiant intensity of 1 watt per square cm. falls on the sample connected as in Fig. 32. This value of course depends on the value of V_0, the dc driving voltage.

Assume $R_L = 1/\bar{G} = \bar{R}$, the dark resistance of the sample.

Then the current change produced by illumination is

$$\Delta I_{sig} = V_o \left[\frac{1}{R + R_L} - \frac{1}{2 R_L} \right]$$

$$= V_o \left[\frac{1}{(1/\bar{G}) + [1/(\bar{G} + \Delta G)]} - \frac{1}{2/\bar{G}} \right]$$

$$= \frac{V_o}{2} \frac{\bar{G}\, \Delta G}{2\bar{G} + \Delta G}$$

$$\Delta I_{sig} \cong \frac{V_o}{4} \Delta G \qquad \text{(A12)}$$

and the voltage change developed across R_L is

$$\Delta V_{sig} = \Delta I_{sig} / \bar{G}$$

$$= \frac{V_o}{4} \frac{\Delta G}{\bar{G}} \qquad \text{(A13)}$$

Thus inserting $\Delta G/\bar{G}$ from Eq. (A10),

$$\Delta V_{sig} = \frac{V_o}{4} \frac{I_o}{\bar{n}} \frac{\tau}{[1 + (\omega\tau)^2]^{1/2}} \left(\frac{1 - e^{-\alpha d}}{d} \right). \qquad \text{(A14)}$$

ACKNOWLEDGEMENTS

This dissertation was supported and encouraged by the Naval Ordnance Laboratory as a part of its program for the advancement of the Laboratory's scientific and technical personnel. I am grateful for this support and encouragement.

I should like to thank the many people who have contributed to this investigation. Dr. W. W. Scanlon guided the experimental phases of the investigation. The interpretation of results has been developed through many helpful discussions with Dr. Scanlon and Dr. R. L. Petritz.

I am indebted to Dr. L. R. Maxwell and Dr. D. F. Bleil for their continued interest and support of the project.

The glass work was prepared by W. E. Clark, H. L. Hoyt, C. W. Teske, and John Huff. Many of the cell design ideas were developed by them. Other members of the Solid State Division and its consultants have contributed by discussion, advice, and assistance at various times throughout the work.

Finally Dr. J. H. McMillen and Dr. R. K. Wangsness of the University of Maryland have both given generously of their time as advisors for this work.

REFERENCES CITED

1. K. Bauer, Ann. d. Phys. 38, 84 (1940)
2. R. F. Brebrick and W. W. Scanlon, Phys. Rev. 96, 598 (1954)
3. R. L. Petritz and W. W. Scanlon, Phys. Rev. 97, 1620 (1955)
4. L. Eisenmann, Ann. d. Phys. 38, 121 (1940)
5. H. Hintenberger, Zeitz. f. Phys. 119, 1 (1942)
6. _____, Zeitz. f. Naturforsch. 1, 12 (1946)
7. D. E. Blackwell, O. Simpson, and G.R.A. Sutherland, Nature, London, 160, 793 (1947)
8. T. S. Moss and R. P. Chasmar, Nature, London, 161, 244 (1948)
9. J. Starkiewicz, J.O.S.A. 38, 481 (1948)
10. T. S. Moss, Proc. Phys. Soc. Lond. B 62, 741 (1949)
11. A. F. Gibson, W. D. Lawson, and T. S. Moss, Proc. Phys. Soc. Lond. A 64, 1054 (1951)
12. N. F. Mott and R. W. Gurney, Electronic Processes in Ionic Crystals, 2nd Edition, Oxford University Press, London, p. 26 (1948)
13. F. L. Lummis and W. W. Scanlon, Navord Report 1899
14. H. K. Henish, Metal Rectifiers, Oxford Univ. Press, London (1949)
15. A. F. Gibson, Proc. Phys. Soc. Lond. B 63, 756 (1950)
16. E. H. Putley and J. E. Arthur, Proc. Phys. Soc. Lond. B 64 (1951)
17. A. F. Gibson, Proc. Phys. Soc. Lond. B 65, 378 (1952)
18. W. W. Scanlon, Phys. Rev. 92, 1573 (1953)
19. D. G. Avery, Proc. Phys. Soc. Lond. B 67, 2 (1954)
20. W. Shockley and W. T. Reed, Jr., Phys. Rev. 87, 835 (1952)

21. H. Y. Fan, D. Navon, and H. Gebbie, Physica 20, 855 (1954)

22. R. A. Smith, Semiconducting Materials, edited by H. K. Henish, Butterworth Publications Ltd., London, p. 204 (1951)

23. A. F. Gibson, Proc. Phys. Soc. Lond. B 64, 603 (1951)

24. R. A. Smith, Physica 20, 910 (1954)

25. D. E. Bode and H. Levinstein, Phys. Rev. 96, 259 (1954)

26. D. G. Avery, reported by R. P. Chasmar, Atlantic City Conference on Photoconductivity (1954), John Wiley & Sons, Inc., New York. In preparation.

27. D. L. Dexter, Ibid.

28. J. Bardeen, F. J. Platt, and L. H. Hall, Ibid.

29. H. Y. Fan, M. L. Shepherd, and E. W. Spitzer, Ibid.

30. R. L. Petritz, Ibid.

NAVORD Report 3922

DISTRIBUTION

	Copies
Chief of Naval Operations, Navy Department Washington 25, D. C. Attn: OP 41 (Materials) OP 317C (Electronics) OP 403 (Planning)	3
Chief, Bureau of Ordnance, Navy Department Washington 25, D. C. Attn: Re4e (P. G. Nutting) Re8-4 (K. V. Knight) Re8c (Mrs. Beggs) Re9a (M. West)	4
Office of Naval Research, Navy Department Washington 25, D. C. Attn: Code 421 Code 427	2
Director, Office of Naval Research, Branch Office 150 Causeway Street, Boston 10, Massachusetts	1
Office of Naval Research, 346 Broadway New York 7, New York	1
Office of Naval Research, American Fore Building 844 North Rush Street, Chicago 11, Illinois	1
Office of Naval Research, 1000 Geary Street San Francisco 24, California	1
Office of Naval Research, 1030 East Green Street Pasadena 1, California	1
Officer in Charge, Office of Naval Research, Branch Office Navy Number 100, Fleet Post Office, New York, New York	1
Director, Naval Research Laboratory Washington 25, D. C. Attn: Code 2020 (Library) Code 6430 (E. Burstein) Code 6450 (S. H. Liebson) Code 7300 (J. A. Sanderson) Code 7350 (H. L. Clark, Optics Division) Technical Information Officer	6

	Copies
Chief, Bureau of Aeronautics, Navy Department Washington 25, D. C. Attn: TD-414 (Technical Data) RS-5 (Research - Physics)	2
Chief, Bureau of Ships, Navy Department Washington 25, D. C. Attn: Code 853 (Mr. Woodside) Code 330 (Materials Research and Development) Code 312 (Technical Library)	3
Naval Ordnance Plant Indianapolis, Indiana Attn: J. Fred Peoples	1
Commander, U. S. Naval Ordnance Test Station Inyokern, China Lake, California Attn: R. S. Witte	1
Naval Electronics Laboratory Technical Information Library, San Diego, California	1
Chief, Engineering and Technical Division Office of the Chief Signal Officer Department of the Army, Washington 25, D. C. Attn: SIGTMS SIGGG-S	2
Office of Chief of Ordnance Research and Development Service Department of the Army, Washington 25, D. C. Attn: ORTX-AR	1
Commanding Officer, Frankford Arsenal Philadelphia 37, Pennsylvania Attn: Fire Control Division	1
Commanding Officer Engineering and Development Laboratories Fort Belvoir, Virginia Attn: Radiation Branch G. E. Brown	2
Commanding Officer, Evans Signal Laboratory Belmar, New Jersey Attn: Applied Physics Branch Physical Optics Section	2

	Copies
Director, Squier Signal Laboratory, SCEL Fort Monmouth, New Jersey Attn: Components and Materials Branch Chemical Physics Branch (S. Benedict Levin)	2
Department of the Army, Chief of Ordnance Research and Development Division, Washington 25, D. C. Attn: ORDTS ORDTR-FAFC ORTX-AR	3
Department of the Army, Technical Branch Scientific Section Department of Defense, Washington 25, D. C. Attn: Dr. L. F. Woodruff	1
U. S. Army, Office of Ordnance Research Box CM, Duke Station, Durham, North Carolina	1
Hq. Air Force, Research and Development Division Department of Defense, Washington 25, D. C. Attn: AFDRD-EL-5	1
Commanding General, Wright Air Development Center Wright-Patterson Air Force Base, Dayton, Ohio Attn: MCREXGO-4, Capt. R. W. Hommel, USAF MCREER-33, P. J. Overbo WCEG	3
Office, U. S. Air Forces, Department of Defense Washington 25, D. C. Attn: AFOIN-IAI	1
Air Research and Development Command, PO Box 1395 Baltimore 3, Maryland	1
Washington Air Force Development Field Office, 4945 Main Navy Building Washington 25, D. C.	1
Armed Services Technical Information Agency Document Service Center, U. B. Building, Dayton, Ohio	1
Director, Naval Ordnance Laboratory Corona, California Attn: Radiometry Section	1
National Research Council, Physical Sciences Division 21st and Constitution Avenue, Washington 25, D. C.	1

	Copies
Library of Congress, Navy Research Section Washington 25, D. C.	1
Document Custodian, Los Alamos Scientific Laboratory Los Alamos, New Mexico	1
Director, Oak Ridge National Laboratory Oak Ridge, Tennessee Attn: Library	1
National Bureau of Standards, Washington, D. C. Attn: E. K. Plyler J. W. Seaton	2
Radio Corporation of America, Princeton, New Jersey Attn: A. Rose E. E. Hahn G. A. Morton	3
Eastman Kodak Company, Rochester, New York Attn: E. D. McAlister C. Koch	2
Philips Laboratories, Inc., Irvington-on-Hudson, New York Attn: E. S. Rittner	1
Photoswitch, Incorporated, 77 Broadway Cambridge 42, Massachusetts Attn: Dr. R. H. McFee	1
National Advisory Committee for Aeronautics Louis Laboratory, Cleveland, Ohio Attn: Library	1
Batelle Memorial Institute, Columbus, Ohio Attn: Solid State Division	1
Polaroid Corporation, Cambridge 39, Massachusetts Attn: R. Clark Jones	1
North American Aviation, Inc., Downey, California Attn: Library	1
Baird Associates, Cambridge, Massachusetts Attn: B. H. Billings	1
Argonne National Laboratory, Bailey and Bluff Lemont Sts. Chicago, Illinois	1

	Copies
Hughes Aircraft Company, Physics Research Department Culver City, California	1
Bell Telephone Laboratories, Murray Hill, New Jersey Attn: Library Mason Clark	2
University of Illinois, Urbana, Illinois Attn: Department of Physics, R. J. Maurer J. Bardeen	2
University of Maryland, College Park, Maryland Attn: Department of Physics, J. F. Singer Institute of Fluid Dynamics, E. W. Montroll	2
Kansas State College, Manhattan, Kansas Attn: C. F. Oakley, Department of Physics	1
University of Pennsylvania, Philadelphia 4, Pennsylvania Attn: Department of Physics, P. H. Miller, Jr. B. Roswell Russell	2
Purdue University, West Lafayette, Indiana Attn: Department of Physics, Karl Lark-Horovitz	1
University of Michigan, Ann Arbor, Michigan Attn: Department of Physics, G. B. B. M. Sutherland	1
University of Michigan, Willow Run Research Center Ypsilanti, Michigan Attn: L. G. Mundie O. L. Tiffany	2
Syracuse University, Syracuse, New York Attn: Department of Physics, H. Levenstein	1
Massachusetts Institute of Technology Cambridge 39, Massachusetts Attn: Laboratory for Insulation Research A. von Hipple Department of Physics, J. C. Slater Department of Electrical Engineering W. Nottingham	3
University of Wisconsin, Madison, Wisconsin Attn: Department of Physics, W. W. Beeman	1
Northwestern University, Evanston, Illinois Attn: Department of Physics, R. J. Cashman	1

	Copies
Johns Hopkins University, Applied Physics Laboratory Silver Spring, Maryland Attn: S. Silverman	1
Director, Brookhaven National Laboratory Upton, Long Island, New York	1
Armour Research Foundation, Illinois Institute of Technology Chicago, Illinois Attn: Calloway Brown	1
University of California, Berkeley, California Attn: C. Kittel	1
Chicago Midway Laboratories, University of Chicago Chicago, Illinois Attn: Eric Durand R. F. Rieke Mrs. M. S. Boche, Librarian	3
National Science Foundation 1520 H Street, N.W. Washington 25, D. C. Attn: J. Howard McMillen	1
Capehart Farnsworth, Solid State Division Fort Wayne, Indiana	1
American Optical Company, Southbridge, Massachusetts Attn: H. Osterberg	1
University of Rochester, Rochester, New York Attn: Institute of Optics, D. L. Dexter	1
Baldwin Piano Company, 1801 Gilbert Avenue Cincinnati 2, Ohio Attn: Dr. W. Love	1
Hycon Manufacturing Company, 2961 E. Colorado Pasadena 8, California Attn: P. W. Shadle	1
Minnesota Mining and Manufacturing Company Highway 12 and East Avenue St. Paul, Minnesota Attn: B. F. Murphey, Central Research Department	1